



**HAL**  
open science

# PHYSICS-BASED BALANCING DOMAIN DECOMPOSITION BY CONSTRAINTS FOR HETEROGENEOUS PROBLEMS

Santiago Badia, Hieu Nguyen

► **To cite this version:**

Santiago Badia, Hieu Nguyen. PHYSICS-BASED BALANCING DOMAIN DECOMPOSITION BY CONSTRAINTS FOR HETEROGENEOUS PROBLEMS. 2016. hal-01337968v2

**HAL Id: hal-01337968**

**<https://hal.science/hal-01337968v2>**

Preprint submitted on 6 Jul 2016 (v2), last revised 27 Nov 2018 (v5)

**HAL** is a multi-disciplinary open access archive for the deposit and dissemination of scientific research documents, whether they are published or not. The documents may come from teaching and research institutions in France or abroad, or from public or private research centers.

L'archive ouverte pluridisciplinaire **HAL**, est destinée au dépôt et à la diffusion de documents scientifiques de niveau recherche, publiés ou non, émanant des établissements d'enseignement et de recherche français ou étrangers, des laboratoires publics ou privés.

# PHYSICS-BASED BALANCING DOMAIN DECOMPOSITION BY CONSTRAINTS FOR HETEROGENEOUS PROBLEMS \*

SANTIAGO BADIA<sup>†‡</sup> AND HIEU NGUYEN<sup>‡</sup>

**Abstract.** In this work, we present a balancing domain decomposition by constraints method based on an aggregation of elements depending on the physical coefficients. Instead of imposing constraints on purely geometrical objects (faces, edges, and vertices) of the partition interface, we use interface objects (subfaces, subedges, and vertices) determined by the variation of the coefficients. The new method is easy to implement and does not require to solve any eigenvalue or auxiliary problem. When the physical coefficient in each object is constant at every subdomain containing the object, we can show both theoretically and numerically that the condition number does not depend on the contrast of the coefficient. The constant coefficient condition is possible for multi-material problems. However, for heterogeneous problems with coefficient varying across a wide spectrum of values in a small spatial scale, such restriction might result in too many objects (a large coarse problem). In this case, we propose a relaxed version of the method where we only require that the maximal contrast of the physical coefficient in each object is smaller than a predefined threshold. The threshold can be chosen so that the condition number is reasonably small while the size of the coarse problem is not too large. An extensive set of numerical experiments is provided to support our findings.

**Key words.** BDDC, heterogeneous problem, adaptive coarse space, parallel solver, parallel preconditioner

**AMS subject classifications.** 65N55, 65N22, 65F08

1     **1. Introduction.** Many realistic simulations in science and engineering, such  
2 as subsurface flow simulations in a nuclear waste repository or in an oil reservoir, or  
3 heat conduction in composites, involve heterogeneous materials. The linear systems  
4 resulting from the discretization of these problems are hard to solve. The use of direct  
5 solvers at a sufficiently fine scale can be prohibitively expensive, even with modern  
6 supercomputers, due to their high complexity and scalability issues. In addition, the  
7 high contrast of the physical properties significantly increases the condition number  
8 of the resulting linear systems, posing great challenges for iterative solvers. In this  
9 work, we will focus on developing a domain decomposition (DD) preconditioner that  
10 is robust with the variation of the coefficients of the PDEs. For a different but related  
11 approach, to find reasonably accurate heterogeneous solution on a coarse mesh, we  
12 refer the interested readers to [19, 1] and references therein.

13     DD is one of the most popular approaches to solve large-scale problems on parallel  
14 supercomputers. It splits a problem into weakly coupled subproblems on smaller  
15 subdomains and use parallel local solutions on these subdomains to form a parallel  
16 preconditioner for the original problem [50, 41]. In DD, the coarse space plays an  
17 important role in achieving scalability as well as robustness w.r.t variations in the  
18 coefficient. Many early DD methods, such as those in [11, 18, 17, 31, 53], work  
19 for heterogeneous problems when the subdomain partition is a geometric coarse grid  
20 that resolves the discontinuities in the properties of the media. This is a strong  
21 requirement, since the properties of the media might have complicated variations

---

<sup>†</sup>Universitat Politècnica de Catalunya, Jordi Girona 1-3, Edifici C1, 08034 Barcelona, Spain.

<sup>‡</sup>CIMNE – Centre Internacional de Mètodes Numèrics en Enginyeria, Parc Mediterrani de la Tecnologia, UPC, Esteve Terradas 5, 08860 Castelldefels, Spain ({sbadia,hnguyen}@cimne.upc.edu).

\*This work has been funded by the European Research Council under the FP7 Program Ideas through the Starting Grant No. 258443 - COMFUS: Computational Methods for Fusion Technology and the FP7 NUMEXAS project under grant agreement 611636. S. Badia gratefully acknowledges the support received from the Catalan Government through the ICREA Acadèmia Research Program.

22 on many scales and be difficult to capture by a geometric coarse grid. Further, it  
23 is impractical, since it would not lead to load-balanced partitions with a reduced  
24 interface.

25 Recently, there have been works on coarse grids that do not resolve the hetero-  
26 geneity in the media [25, 45, 25, 43, 44], and especially automatic coarse spaces that  
27 adapt to the variation in the properties of the media [22, 23, 42, 47, 15, 49, 48, 28,  
28 27, 29, 36, 24]. In the latter, the coarse spaces are constructed from eigenfunctions  
29 associated with small eigenvalues (low-frequency modes) of appropriated generalised  
30 eigenvalue problems. This approach is backed up by rigorous mathematical theory  
31 and has been numerically shown to be robust for general heterogeneous problems.  
32 However, solving eigenvalue problems is expensive and extra implementation effort is  
33 required as coarse spaces in DD methods are not naturally formulated as eigenfunc-  
34 tions. Another approach is to use the deluxe scaling technique where local auxiliary  
35 Dirichlet problems are solved to compute efficient averaging operators [33, 14, 52].  
36 The approach yields robust DD methods, but extra implementation and computation  
37 cost incur due to the auxiliary problems. In this paper, we formulate a *new balancing*  
38 *DD by constraints (BDDC) preconditioner that requires no eigenvalue or auxiliary*  
39 *problem and is very robust with the contrast of the coefficient.* The main motivation  
40 behind this work is to achieve such goal while *maintaining the simplicity* of the BDDC  
41 preconditioner.

42 The BDDC method was introduced by Dohrmann in 2003 [12]. It is an improved  
43 version of the balancing DD (BDD) method by Mandel [38] and has a close connection  
44 with the FETI-DP method [21, 20]. In fact, it can be shown that the eigenvalues  
45 of the preconditioned operators associated with BDDC and FETI-DP are almost  
46 identical [39, 34, 10]. The BDDC method is particularly well-suited for extreme scale  
47 simulations, since it allows for a very aggressive coarsening, the computations at  
48 different levels can be computed in parallel, the subdomain problems can be solved  
49 inexactly [13, 35] by, e.g., one AMG cycle, and it can straightforwardly be extended  
50 to multiple levels [51, 40]. All of these properties have been carefully exploited in  
51 the series of articles [3, 4, 5, 6] where an extremely scalable implementation of these  
52 algorithms has been proposed, leading to excellent weak scalability on nearly half a  
53 million cores in its multilevel version.

54 Our new BDDC method is motivated from the fact that non-overlapping DD  
55 methods, such as BDDC and FETI-DP, are robust with the variation and contrast  
56 of the coefficient if it is constant (or varies mildly) in each subdomain [31, 30, 50].  
57 This implies that in order to have robustness for BDDC methods one could use a  
58 physics-based partition obtained by aggregating elements of the same coefficient value.  
59 However, using this type of partition is impractical as the number of the subdomains  
60 might be too large and can lead to a poor load balancing among subdomains and  
61 large interfaces. In order to solve this dilemma, we propose to use a well-balanced  
62 partition, e.g., one obtained from METIS [26] an automatic graph partitioner, to  
63 distribute the work load among processors. Then, we consider a sub-partition of sub-  
64 domains based on the physical coefficients, leading to a physic-based (PB) partition.  
65 Continuity constraints among subdomains will be defined through the definition of  
66 objects based on the PB partition. Consequently, the interface objects are adaptively  
67 defined according to the variation of the coefficient. The resulting BDDC pre-  
68 conditioner with constraints imposed on subfaces, subedges, and vertices will be called  
69 PB-BDDC. These ideas can readily be applied to FETI-DP preconditioners.

70 We emphasise that the PB-BDDC method does not require to solve any eigenvalue  
71 or auxiliary problems. Its formulation and implementation are very much the same

72 as for the standard BDDC method. The only difference is in identifying and defining  
 73 BDDC objects to impose constraints. In other words, *the simplicity of the standard*  
 74 *BDDC method is maintained.*

75 For multi-material problems, e.g., problems with isolated channels or inclusions,  
 76 it is possible to require the physical coefficient in each PB-subdomain to be constant.  
 77 In this situation, we are able to prove that *the new BDDC method is scalable and its*  
 78 *convergence is independent of the contrast of the coefficient.*

79 For heterogeneous problems with a wide spectrum of values in a small spatial  
 80 scale this restriction is too strong and might result in too many coarse objects (large  
 81 coarse problem). As a result, we also propose a relaxed definition of the PB partition  
 82 where we only require that the maximal contrast of the physical coefficient in each  
 83 PB-subdomain is smaller than a predefined threshold. The threshold can be chosen  
 84 so that the condition number is reasonably small while the size of the coarse problem  
 85 is not too large. We empirically show that this relaxed version of PB-BDDC, called  
 86 rPB-BDDC, is robust and efficient for different difficult distributions of the coefficient.

87 The rest of the paper is organised as follows. In [section 2](#), we introduce the model  
 88 problem, the domain partitions and the BDDC object classification. In [section 3](#), we  
 89 present the formulation of the (r)PB-BDDC methods as well as their key ingredients,  
 90 namely coarse degrees of freedom (coarse DOFs), weighting and harmonic extension  
 91 operators. The convergence analysis is also provided in this section. In [section 4](#),  
 92 we provide an extensive set of numerical experiments to demonstrate the robustness  
 93 and efficiency of the (r)PB-BDDC methods. We finally draw some conclusions in  
 94 [section 5](#).

95 **2. Problem setting.** Let  $\Omega \subset \mathbb{R}^d$ , with  $d$  being the space dimension, be a  
 96 bounded polyhedral domain. For a model problem, we study the Poisson's equa-  
 97 tion with non-constant diffusion and homogeneous Dirichlet conditions (the non-  
 98 homogeneous case only involves an obvious modification of the right-hand side). Thus,  
 99 the problem at hand is: find  $u \in H_0^1(\Omega)$  such that  $-\alpha \Delta u = f$  in  $H^{-1}(\Omega)$  sense, with  
 100  $f \in H^{-1}(\Omega)$  and  $\alpha \in L^\infty(\Omega)$  strictly positive. The weak form of the problem reads  
 101 as: find  $u^* \in H_0^1(\Omega)$  such that

$$102 \quad (1) \quad \int_{\Omega} \alpha \nabla u^* \cdot \nabla v \, dx = \int_{\Omega} f v \, dx, \quad \text{for any } v \in H_0^1(\Omega).$$

103 Let  $\mathcal{T}$  be a shape-regular quasi-uniform mesh of  $\Omega$  with characteristic size  $h$ . It can  
 104 consist of tetrahedra or hexahedra for  $d = 3$ , or triangles or quadrilaterals for  $d = 2$ .  
 105 For simplicity of exposition, we assume that  $\alpha$  is constant on each element  $\tau \in \mathcal{T}$ .

106 **2.1. Domain partitions.** We first consider a partition  $\Theta$  of  $\Omega$  into non-overlapping  
 107 open subdomains. This partition must be driven by computational efficiency in dis-  
 108 tributed memory platforms, i.e., it should have a reduced interface size and lead to  
 109 a well-balanced distribution of work load among processors. In a parallel implemen-  
 110 tation, each subdomain in  $\Theta$  is generally assigned to a processor. We further assume  
 111 that every  $\mathcal{D} \in \Theta$  can be obtained by *aggregation of elements* in  $\mathcal{T}$  and is connected.  
 112 We denote by  $\Gamma(\Theta)$  the interface of the partition  $\Theta$ , i.e.,  $\Gamma(\Theta) \doteq (\cup_{\mathcal{D} \in \Theta} \partial \mathcal{D}) \setminus \partial \Omega$ .

113 We also consider a PB subdomain partition. This partition is used latter in the  
 114 new definition of coarse objects and in the analysis. It is, however, not used for work  
 115 distribution. Given a subdomain  $\mathcal{D} \in \Theta$ , we can further consider its partition  $\Theta_{\text{pb}}(\mathcal{D})$   
 116 into a set of “sub-subdomains” with constant  $\alpha$ . The minimal set is preferred for  
 117 efficiency (it will potentially lead to a smaller coarse space) but it is not a requirement  
 118 (see [Remark 5](#)). Clearly, the resulting global PB partitions  $\Theta_{\text{pb}} \doteq \{\Theta_{\text{pb}}(\mathcal{D})\}_{\mathcal{D} \in \Theta}$

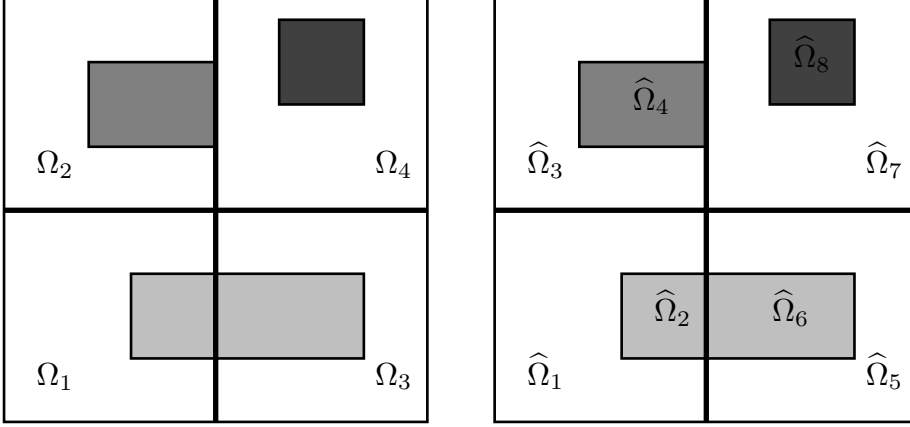


FIG. 1. An example of an original partition  $\Theta$  (left) and a physics-based partition  $\Theta_{\text{pb}}$  (right) of a square domain where different colors represent different values of  $\alpha$ . On the left, we have a  $\Theta = \{\Omega_1, \Omega_2, \Omega_3, \Omega_4\}$ . On the right, we show the corresponding PB-partition for every subdomains in  $\Theta$ :  $\Theta_{\text{pb}}(\Omega_1) = \{\hat{\Omega}_1, \hat{\Omega}_2\}$ ,  $\Theta_{\text{pb}}(\Omega_2) = \{\hat{\Omega}_3, \hat{\Omega}_4\}$ ,  $\Theta_{\text{pb}}(\Omega_3) = \{\hat{\Omega}_5, \hat{\Omega}_6\}$ , and  $\Theta_{\text{pb}}(\Omega_4) = \{\hat{\Omega}_7, \hat{\Omega}_8\}$ . The complete PB-partition is  $\Theta_{\text{pb}} = \{\hat{\Omega}_1, \dots, \hat{\Omega}_8\}$ . Further, we have  $\omega(\hat{\Omega}_1) = \omega(\hat{\Omega}_2) = \Omega_1$ ,  $\omega(\hat{\Omega}_3) = \omega(\hat{\Omega}_4) = \Omega_2$ ,  $\omega(\hat{\Omega}_5) = \omega(\hat{\Omega}_6) = \Omega_3$ ,  $\omega(\hat{\Omega}_7) = \omega(\hat{\Omega}_8) = \Omega_4$ .

119 is also a partition of  $\Omega$  (into PB subdomains). The interface of this partition is  
 120  $\Gamma(\Theta_{\text{pb}}) \doteq (\cup_{\hat{\mathcal{D}} \in \Theta_{\text{pb}}} \partial \hat{\mathcal{D}}) \setminus \partial \Omega$ . For a subdomain  $\mathcal{D} \in \Theta$  (analogously for  $\hat{\mathcal{D}} \in \Theta_{\text{pb}}$ ), we  
 121 denote by  $\mathcal{T}_{\mathcal{D}}$  the submesh of  $\mathcal{T}$  associated with  $\mathcal{D}$ ,  $\mathcal{T}_{\mathcal{D}} \doteq \{\tau \in \mathcal{T} : \tau \subset \mathcal{D}\} \subset \mathcal{T}$ . For  
 122 any  $\hat{\mathcal{D}} \in \Theta_{\text{pb}}$ , let  $\omega(\hat{\mathcal{D}})$  be the only subdomain in  $\Theta$  that contains  $\hat{\mathcal{D}}$ . In Figure 1, we  
 123 show an example of the original partition  $\Theta$  and the PB partition  $\Theta_{\text{pb}}$  for a simple  
 124 problem. The meaning of  $\Theta_{\text{pb}}(\mathcal{D})$  and  $\omega(\mathcal{D})$  is also illustrated.

125 **2.2. Finite element spaces.** Let us perform a discretization of (1) by a con-  
 126 tinuous finite element (FE) space  $\bar{\mathbb{V}}$  associated with the mesh  $\mathcal{T}$ . The discontinuous  
 127 Galerkin (DG) case will not be considered in this work, but we refer the reader to  
 128 [16] for more information.

129 For every subdomain  $\mathcal{D} \in \Theta$ , we consider a FE space  $\mathbb{V}_{\mathcal{D}}$  associated with the  
 130 local mesh  $\mathcal{T}_{\mathcal{D}}$ . Let  $H(\mathcal{D})$  be the characteristic length of the subdomain  $\mathcal{D}$  and  $h(\mathcal{D})$   
 131 be the characteristic length of the FE mesh  $\mathcal{T}_{\mathcal{D}}$ . We define the Cartesian product of  
 132 local FE spaces as  $\mathbb{V} = \prod_{\mathcal{D} \in \Theta} \mathbb{V}_{\mathcal{D}}$ . We note that functions in this space are allowed to  
 133 be discontinuous across the interface  $\Gamma(\Theta)$ . Clearly,  $\bar{\mathbb{V}} \subset \mathbb{V}$ .

134 For a subdomain  $\mathcal{D} \in \Theta$ , we also define the subdomain FE operator  $\mathcal{A}_{\mathcal{D}} : \mathbb{V}_{\mathcal{D}} \rightarrow$   
 135  $\mathbb{V}'_{\mathcal{D}}$  as  $\langle \mathcal{A}_{\mathcal{D}} u, v \rangle \doteq \int_{\mathcal{D}} \alpha \nabla u \cdot \nabla v \, dx$ , for all  $u, v \in \mathbb{V}_{\mathcal{D}}$ , and the sub-assembled operator  
 136  $\mathcal{A}^{\Theta} : \mathbb{V} \rightarrow \mathbb{V}'$  as  $\langle \mathcal{A}^{\Theta} u, v \rangle \doteq \sum_{\mathcal{D} \in \Theta} \langle \mathcal{A}_{\mathcal{D}} u, v \rangle$ , for all  $u, v \in \mathbb{V}$ .

137 A function  $u \in \mathbb{V}_{\mathcal{D}}$  is said to be discrete  $\alpha$ -harmonic in  $\mathcal{D}$  if

$$138 \quad \langle \mathcal{A}_{\mathcal{D}} u, v \rangle = 0, \quad \text{for any } v \in \mathbb{V}_{0, \mathcal{D}},$$

139 where  $\mathbb{V}_{0, \mathcal{D}} \doteq \{v \in \mathbb{V}_{\mathcal{D}} : v = 0 \text{ on } \partial \mathcal{D}\}$ . It should be noted that if  $u$  is discrete  
 140  $\alpha$ -harmonic in  $\mathcal{D}$  then it satisfies the energy minimising property, namely

$$141 \quad \langle \mathcal{A}_{\mathcal{D}} u, u \rangle \leq \langle \mathcal{A}_{\mathcal{D}} v, v \rangle, \quad \forall v \in \mathbb{V}_{\mathcal{D}}, v|_{\partial \mathcal{D}} = u|_{\partial \mathcal{D}}.$$

142 In addition, we consider the assembled operator  $\mathcal{A} : \bar{\mathbb{V}} \rightarrow \bar{\mathbb{V}}'$ , defined by  $\langle \mathcal{A} u, v \rangle =$   
 143  $\int_{\Omega} \alpha \nabla u \cdot \nabla v \, dx$ , for all  $u, v \in \bar{\mathbb{V}}$ . This operator is the Galerkin projection of  $\mathcal{A}^{\Theta}$  onto

144  $\bar{\mathbb{V}}$ . We want to compute a FE approximation  $u \in \bar{\mathbb{V}}$  of  $u^*$  in (1) such that

145 (2)  $\langle \mathcal{A}u, v \rangle = \langle f, v \rangle, \quad \text{for any } v \in \bar{\mathbb{V}}.$

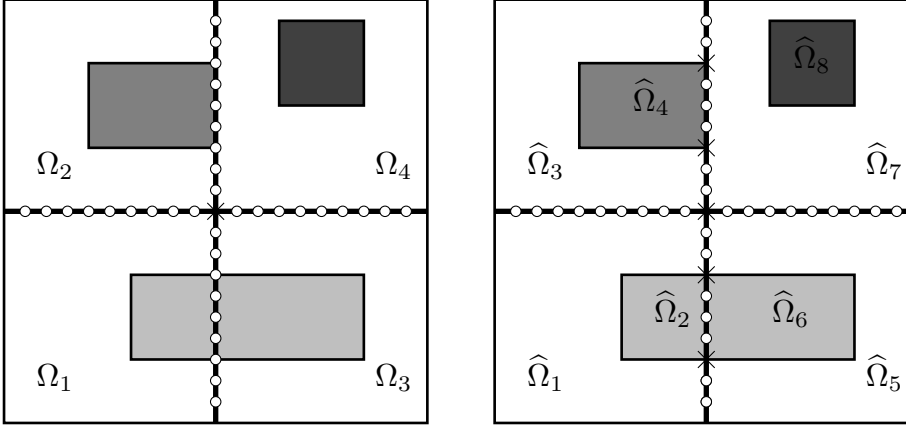


FIG. 2. An example of how FE nodes (on the interface of the original partition  $\Theta$  in Figure 1) are classified in the standard way (left) using  $\text{neigh}_{\Theta}$ , and in the physics-based way (right) using  $\text{neigh}_{\Theta_{\text{pb}}}$ . Corner nodes are marked with crosses while nodes in edges are marked with small circles. Using the standard classification, on the left, we obtain  $\Lambda(\Theta)$  with one corner and four edges. With the new classification, on the right, we have  $\Lambda_{\text{pb}}(\Theta)$  with five corners and six edges (eight edges if we only consider connected objects).

146 **2.3. Object classification.** This subsection concerns with objects on subdo-  
 147 main interfaces and their classification. It provides foundations for the definition of  
 148 coarse DOFs in BDDC methods later on.

149 Given a subdomain partition  $\Theta$ , and a point  $\xi \in \Gamma(\Theta)$ , let us denote by  $\text{neigh}_{\Theta}(\xi)$   
 150 the set of subdomains in  $\Theta$  that contain  $\xi$ . We can introduce the concept of objects  
 151 as a classification of points in  $\Gamma(\Theta)$ . A *geometrical object* is a maximal set  $\lambda$  of points  
 152 in  $\Gamma(\Theta)$  with identical subdomain set. We denote by  $\text{neigh}_{\Theta}(\lambda)$  the set of subdomains  
 153 in  $\Theta$  containing  $\lambda$ . It should be noted that the set of all geometrical objects, denoted  
 154 by  $\Lambda(\Theta)$ , is a partition of  $\Gamma(\Theta)$ .

155 *Remark 1.* Since the set of points in the interface is infinite, the previous classi-  
 156 fication of  $\Gamma(\Theta)$  into geometrical objects is performed in practice by the classification  
 157 of vertices, edges, and faces of elements in the mesh  $\mathcal{T}$  based on their subdomain set.

158 Denote by  $\text{ndof}(\lambda)$  the number of DOFs belonging to  $\lambda$ . We further consider the  
 159 following standard classification of geometrical objects. In the three-dimensional case,  
 160  $\lambda \in \Lambda(\Theta)$  is a *face* if  $|\text{neigh}_{\Theta}(\lambda)| = 2$  and  $\text{ndof}(\lambda) > 1$ , is an *edge* if  $|\text{neigh}_{\Theta}(\lambda)| > 2$  and  
 161  $\text{ndof}(\lambda) > 1$ , and is a *corner* if  $\text{ndof}(\lambda) = 1$ . In the two-dimensional case,  $\lambda \in \Lambda(\Theta)$   
 162 is an *edge* if  $|\text{neigh}_{\Theta}(\lambda)| = 2$  and  $\text{ndof}(\lambda) > 1$ , and is a *corner* if  $\text{ndof}(\lambda) = 1$ . In the  
 163 literature, e.g. [31, 50], corners are also referred to as vertices. Analogous definitions  
 164 are also used frequently for FETI-DP methods (see [50]). In Figure 2 (left), an  
 165 illustration of this classification is shown for a simple example.

166 In the next step, we define PB objects, which is the main ingredient of the PB-  
 167 BDDC methods proposed herein. We consider the set of objects  $\Lambda_{\text{pb}}(\Theta)$  obtained  
 168 by applying the previous classification of  $\Gamma(\Theta)$  into corners/edges/faces but with  
 169  $\text{neigh}_{\Theta}(\cdot)$  replaced by  $\text{neigh}_{\Theta_{\text{pb}}}(\cdot)$ . In other words, we use sets of subdomains in

170  $\Theta_{\text{pb}}$  to classify geometrical objects on  $\Gamma(\Theta)$ . **Figure 2** (right) shows objects in  $\Lambda_{\text{pb}}(\Theta)$   
 171 for a simple example.

172 **LEMMA 2.**  $\Lambda_{\text{pb}}(\Theta)$  is a refinement of  $\Lambda(\Theta)$ .

173 *Proof.* The statement holds if for every object  $\lambda_{\text{pb}} \in \Lambda_{\text{pb}}(\Theta)$  there exists one and  
 174 only one object  $\lambda \in \Lambda(\Theta)$  containing it. Since all points in  $\lambda_{\text{pb}}$  belong to the same set  
 175 of PB subdomains,  $\text{neigh}_{\Theta_{\text{pb}}}(\lambda)$ , they are in the same set of subdomains in  $\Theta$ , namely  
 176  $\{\omega(\hat{\mathcal{D}})\}_{\hat{\mathcal{D}} \in \text{neigh}_{\Theta_{\text{pb}}}(\lambda)}$ . As a result, all these points belong to the same object in  $\Lambda(\Theta)$ .  $\square$

177 **Remark 3.** In some cases, the DOF-based classification into corners, edges, and  
 178 faces might need some modification in order to ensure well-posedness of the BDDC  
 179 method with corner constraints only. This usually involves the use of a kernel detection  
 180 mechanism (see, e.g, [46]). A new approach based on perturbations has recently been  
 181 proposed in [8, 7], where the method is well-posed in all cases.

182 **Remark 4.** The PB aggregation (classification) of the interface  $\Gamma(\Theta)$  into  $\Lambda_{\text{pb}}(\Theta)$   
 183 can be relaxed. As it is currently stated, the PB partition is unique and have the min-  
 184 imal number of PB subdomains. However, it might introduces disconnected objects.  
 185 For example, the edge between  $\hat{\Omega}_3$  and  $\hat{\Omega}_7$  in **Figure 2** (right) is disconnected. Alter-  
 186 natively, one can require that objects must be connected. This leads to two connected  
 187 edges between  $\hat{\Omega}_3$  and  $\hat{\Omega}_7$ . We adopt this practice for the numerical experiments in  
 188 **section 4**. However, it should be noted that the use of disconnected objects leads to  
 189 a smaller coarse space and can be beneficial in some cases.

190 **Remark 5.** In practical implementations, one only needs the set of PB geometrical  
 191 objects  $\Lambda_{\text{pb}}(\Theta)$  to define the PB-BDDC preconditioner. When using the approach  
 192 with only connected objects (see **Remark 4**), one does not need to explicitly define  
 193 the PB partition  $\Theta_{\text{pb}}$ . Only a partition of objects in  $\Lambda(\Theta)$  (see **Figure 2** (left)) into PB  
 194 objects (see **Figure 2** (right)) based on the physical coefficients is required. Therefore,  
 195 only a  $(d - 1)$ -dimensional PB partition (of the interface  $\Gamma(\Theta)$ ) is needed. This is  
 196 what we have actually implemented for our numerical experiments in **section 4**. We  
 197 only use the PB partition  $\Theta_{\text{pb}}$  in the analysis in **subsection 3.4**. In any case, the PB  
 198 partition can easily be implemented if necessary.

199 **3. Physics-based BDDC preconditioning.** In this section, we present our  
 200 new PB-BDDC method. The basic idea behind BDDC methods is first to define a  
 201 sub-assembled operator (no assembling among subdomains), and the global space of  
 202 functions that are fully independent (“discontinuous”) among subdomains. Secondly,  
 203 we have to define the under-assembled space (the BDDC space) of functions for which  
 204 continuity among subdomains is enforced only on a set of coarse DOFs. In order to  
 205 be robust for heterogeneous problems, the PB-BDDC method utilises new definitions  
 206 of the BDDC space (i.e., new coarse DOF continuity among subdomains) and a new  
 207 weighting operator.

208 **3.1. Coarse degrees of freedom.** Similarly to other BDDC methods, in the  
 209 PB-BDDC method, some (or all) of the objects in  $\Lambda_{\text{pb}}(\Theta)$  are associated with a  
 210 coarse DOF. We denote this set of objects by  $\Lambda_O$  and call it the set of coarse objects.  
 211 Obviously,  $\Lambda_O \subset \Lambda_{\text{pb}}(\Theta)$ . Typical choices of  $\Lambda_O$  are  $\Lambda_O \doteq \Lambda_C$ , when only corners  
 212 are considered,  $\Lambda_O \doteq \Lambda_C \cup \Lambda_E$ , when corners and edges are considered, or  $\Lambda_O \doteq$   
 213  $\Lambda_{\text{pb}}(\Theta)$ , when corners, edges, and faces are considered. These choices lead to three  
 214 variants of the PB-BDDC method, referred to as PB-BDDC(c), PB-BDDC(ce) and  
 215 PB-BDDC(cef), respectively. **Figure 2** (right) actually shows the coarse objects of  
 216 PB-BDDC(ce) for a simple 2D problem.

217 Given an object  $\lambda \in \Lambda_O$ , we define its coarse DOF as the mean value on  $\lambda$ . The  
 218 rigorous definition is as follows. Assume  $\lambda \in \Lambda_O$  is associated with a subdomain  
 219  $\mathcal{D} \in \Theta$ . We define the coarse DOF  $c_\lambda^{\mathcal{D}}$  corresponding to  $\lambda$  as

$$220 \quad (3) \quad c_\lambda^{\mathcal{D}}(u_{\mathcal{D}}) \doteq \frac{\int_\lambda u_{\mathcal{D}} ds}{\int_\lambda 1 ds}, \quad \text{for } u_{\mathcal{D}} \in \mathbb{V}_{\mathcal{D}}.$$

221 Clearly,  $c_\lambda^{\mathcal{D}}$  is a functional in  $\mathbb{V}'_{\mathcal{D}}$ . When  $\lambda$  is a corner,  $c_\lambda^{\mathcal{D}}$  is simply the value at that  
 222 corner. Once we have defined the coarse DOFs, we can define the BDDC space as  
 223 follows

$$224 \quad (4) \quad \tilde{\mathbb{V}} \doteq \{v \in \mathbb{V} : c_\lambda^{\mathcal{D}}(v) = c_\lambda^{\mathcal{D}'}(v), \forall \lambda \in \Lambda_O, \forall \mathcal{D}, \mathcal{D}' \in \text{neigh}_\Theta(\lambda)\},$$

225 i.e., the subspace of functions in  $\mathbb{V}$  that are continuous ‘‘at’’ coarse DOFs. Clearly,  
 226  $\tilde{\mathbb{V}} \subset \bar{\mathbb{V}} \subset \mathbb{V}$ .

227 For BDDC methods, solving the coarse problem is usually the bottleneck (cf.  
 228 [2, 3, 4, 8]). Therefore, it is of great interest to find a minimal set of coarse objects  
 229 (the number of the coarse objects is the number of the coarse DOFs and also is the  
 230 size of the coarse problem), so that BDDC methods can achieve their potential of  
 231 fast convergence and perfect weak scalability. According to [31, 50], in the case where  
 232 the physical coefficient in each subdomain is constant, the set of coarse objects only  
 233 need to guarantee the existence of the so-called *acceptable paths*. We need a similar  
 234 concept here for the PB-BDDC method.

235 The definition below is modelled after [50, Definition 6.26], [31] and [32].

236 **DEFINITION 6** (Acceptable path). *Let  $\Theta_{\text{pb}}^\partial$  be the set of PB subdomains  $\hat{\mathcal{D}} \in \Theta_{\text{pb}}$   
 237 touching the interface  $\Gamma(\Theta)$ , i.e.,  $\partial\hat{\mathcal{D}} \cap \Gamma(\Theta) \neq \emptyset$ . For two subdomains  $\hat{\mathcal{D}}_a, \hat{\mathcal{D}}_b \in \Theta_{\text{pb}}^\partial$   
 238 that share an edge  $\lambda$  but no face in  $\Lambda_{\text{pb}}(\Theta)$  or share a corner  $\lambda$  but no edge in  $\Lambda_{\text{pb}}(\Theta)$ ,  
 239 an acceptable path is a sequence  $\{\hat{\mathcal{D}}_a = \hat{\mathcal{D}}_1, \hat{\mathcal{D}}_2, \dots, \hat{\mathcal{D}}_n = \hat{\mathcal{D}}_b\}$  of PB subdomains in  
 240  $\Theta_{\text{pb}}^\partial$ , which satisfy the following properties:*

- 241 *i) they all share the common object  $\lambda \in \Lambda_{\text{pb}}(\Theta)$*
- 242 *ii) subdomains  $\hat{\mathcal{D}}_k$  and  $\hat{\mathcal{D}}_{k+1}$ ,  $k = 1, \dots, \hat{n} - 1$ , must share, apart from  $\lambda$ , an object*  
 243 *in  $\Lambda_O$  and the type of the shared object (face, edge or corner) must be the same*  
 244 *for the whole sequence*
- 245 *iii) their (constant) coefficients satisfy*

$$246 \quad \text{TOL } \alpha_k \geq R(k, \lambda) \min(\alpha_a, \alpha_b), \quad 1 \leq k \leq n$$

247 *where TOL is some predefined tolerance and  $R(k, \lambda) = 1$  if  $\lambda$  is an edge and*  
 248  *$R(k, \lambda) = h(\hat{\mathcal{D}}_k)/H(\hat{\mathcal{D}}_k)$  if  $\lambda$  is a corner.*

249 **Assumption 7.** We assume that the set of BDDC objects  $\Lambda_O$  satisfies the following  
 250 properties:

- 251 1. In the three dimensional case, for each face on  $\Gamma(\Theta)$ , there is at least one edge  
 252 that is part of its boundary and belongs to  $\Lambda_O$ .
- 253 2. For all pairs of subdomains  $\hat{\mathcal{D}}_a, \hat{\mathcal{D}}_b \in \Theta_{\text{pb}}^\partial$ , which have an edge but not a face  
 254 in  $\Lambda_{\text{pb}}(\Theta)$  in common, or a corner but not an edge in  $\Lambda_{\text{pb}}(\Theta)$  in common,  
 255 there exists an acceptable path for a predefined tolerance TOL.

256 **Remark 8.** In **Definition 6**, if the shared object  $\lambda$  belongs to the set of BDDC  
 257 objects  $\Lambda_O$ , then there exists a trivial acceptable path  $\{\hat{\mathcal{D}}_a, \hat{\mathcal{D}}_b\}$  with TOL = 1 and  
 258  $n = 2$ . Thus, BDDC(ce) and BDDC(cef) always satisfy **Assumption 7** for TOL = 1.

259 **3.2. Injection operators.** Let us define the projection  $\mathcal{Q} : \mathbb{V} \rightarrow \bar{\mathbb{V}}$  as some  
 260 weighted average of interface values together with an  $\alpha$ -harmonic extension to sub-  
 261 domain interiors (see, e.g., [39]). We define these ingredients as follows.

262 For  $u \in \mathbb{V}$  and  $\xi \in \Gamma(\Theta)$ , the weighting operator is defined as

$$263 \quad (5) \quad \mathcal{W}u(\xi) \doteq \sum_{\mathcal{D} \in \text{neigh}_{\Theta}(\xi)} \delta_{\mathcal{D}}^{\dagger}(\xi) u_{\mathcal{D}}(\xi), \quad \text{with } \delta_{\mathcal{D}}^{\dagger}(\xi) \doteq \frac{\sum_{\tau \in \mathcal{T}_{\mathcal{D}}, \tau \ni \xi} \alpha_{\tau} |\tau|}{\sum_{\tau \in \mathcal{T}, \tau \ni \xi} \alpha_{\tau} |\tau|},$$

264 where  $|\tau|$  denotes the volume (area if in 2D) of the element  $\tau$ .

265 The  $\alpha$ -harmonic extension operator  $\mathcal{E}$  taking data on the interface  $\Gamma(\Theta)$  and  $\alpha$ -  
 266 harmonically extending it to each subdomain  $\mathcal{D} \in \Theta$  is formally defined as

$$267 \quad \mathcal{E}u \doteq (1 - \mathcal{A}_0^{-1} \mathcal{A})u,$$

268 where  $\mathcal{A}_0$  is the Galerkin projection of  $\mathcal{A}$  onto the bubble space  $\mathbb{V}_0 \doteq \{v \in \mathbb{V} : v =$   
 269  $0 \text{ on } \Gamma(\Theta)\}$ .

270 We finally define  $\mathcal{Q} = \mathcal{E}\mathcal{W}$ .

271 **3.3. PB-BDDC preconditioner.** In this subsection, we present the PB-BDDC  
 272 preconditioner, and describe its set-up and formulation. The PB-BDDC precondi-  
 273 tioner is a BDDC preconditioner in which the set of coarse DOFs enforce continuity  
 274 on a set of PB coarse objects, thus modifying the BDDC space being used. Once one  
 275 has defined the set of PB coarse objects  $\Lambda_{\mathcal{O}}$ , the rest of ingredients of the PB-BDDC  
 276 preconditioner are identical to the ones of a standard BDDC preconditioner. In any  
 277 case, the definition of the weighting operator introduced in (5) is new.

278 The BDDC preconditioner is a Schwarz-type preconditioner that combines interior  
 279 corrections with corrections in the BDDC space (see, e.g., [9, 50]). In case of the PB-  
 280 BDDC preconditioner, the BDDC correction is expressed as  $\mathcal{Q}(\tilde{\mathcal{A}}^{\Theta})^{-1} \mathcal{Q}^T$ , where  $\tilde{\mathcal{A}}^{\Theta}$  is  
 281 the Galerkin projection of  $\mathcal{A}^{\Theta}$  onto  $\bar{\mathbb{V}}$ . More specifically, the PB-BDDC preconditioner  
 282 reads as follows:

$$283 \quad \mathcal{B} = \mathcal{A}_0^{-1} + \mathcal{Q}(\tilde{\mathcal{A}}^{\Theta})^{-1} \mathcal{Q}^T.$$

284 Apart from the task of identifying and defining coarse objects, the implementation  
 285 of the PB-BDDC method is identical to that of the standard BDDC method. We  
 286 refer the interested reader to [12, 13, 40, 9] for more details on the formulation of  
 287 BDDC methods and to [2, 4, 6] for an efficient implementation of BDDC methods on  
 288 distributed memory machines, which requires much further elaboration.

289 **3.4. Condition number estimates.** In order to prove condition number esti-  
 290 mates for the PB-BDDC preconditioner, we first need to introduce  $\hat{\mathcal{B}}$ , an auxiliary  
 291 BDDC preconditioner. The definition of this preconditioner follows verbatim that  
 292 of the PB-BDDC preconditioner above but the PB subdomain partition  $\Theta_{\text{pb}}$  is used  
 293 instead of  $\Theta$ .

294 Given the FE mesh  $\mathcal{T}$ , the FE space type, and the subdomain partition  $\Theta_{\text{pb}}$ , one  
 295 can similarly build the FE spaces and operators as in subsection 2.2, leading to the  
 296 sub-assembled space  $\mathbb{V}^{\text{pb}}$  and operator  $\mathcal{A}^{\Theta_{\text{pb}}}$ . Further, we can define the injection  
 297 operator  $\hat{\mathcal{Q}}$  using the definitions in subsection 3.2 with  $\Theta$  is replaced by  $\Theta_{\text{pb}}$  for the  
 298 weighting  $\hat{\mathcal{W}}$  and harmonic extension  $\hat{\mathcal{E}}$  operators.

299 **LEMMA 9.** *For any PB subdomain  $\hat{\mathcal{D}} \in \Theta_{\text{pb}}$ , the function  $\delta_{\hat{\mathcal{D}}}^{\dagger}(\cdot)$  is constant on*  
 300 *each PB object  $\lambda$  associated with it, i.e.,*

$$301 \quad (6) \quad \delta_{\hat{\mathcal{D}}}^{\dagger}(\xi) = \delta_{\hat{\mathcal{D}}}^{\dagger}(\xi'), \quad \forall \xi, \xi' \in \lambda.$$

302 In addition, the following important inequality, cf. [50, 6.19], holds

$$303 \quad (7) \quad \alpha_{\widehat{\mathcal{D}}_a} \left( \delta_{\widehat{\mathcal{D}}_b}^\dagger(\xi) \right)^2 \leq C_{\delta^\dagger} \min \left( \alpha_{\widehat{\mathcal{D}}_a}, \alpha_{\widehat{\mathcal{D}}_b} \right), \quad \forall \widehat{\mathcal{D}}_a, \widehat{\mathcal{D}}_b \in \text{neigh}_{\Theta_{\text{pb}}}(\xi),$$

304 where  $C_{\delta^\dagger} \lesssim \max \left( 1, \frac{N_{\max}-1}{4} \right)$  with  $N_{\max}$  is the maximal number of elements in  $\mathcal{T}$   
 305 sharing at least one point.

306 *Proof.* The identity (6) follows from (5), the fact that  $\alpha$  is constant in each sub-  
 307 domain in  $\Theta_{\text{pb}}$  and  $\text{neigh}_{\Theta_{\text{pb}}}(\xi) = \text{neigh}_{\Theta_{\text{pb}}}(\xi') = \text{neigh}_{\Theta_{\text{pb}}}(\lambda)$ .

308 Now we need to verify (7). Since  $\alpha$  is constant in each PB subdomain, we can  
 309 rewrite and bound  $\delta_{\widehat{\mathcal{D}}}^\dagger(\xi)$  as follows

$$310 \quad (8) \quad \delta_{\widehat{\mathcal{D}}_b}^\dagger(\xi) = \frac{\alpha_{\widehat{\mathcal{D}}_b} A_{\widehat{\mathcal{D}}_b}}{\sum_{\widehat{\mathcal{D}} \in \text{neigh}_{\text{pb}}(\xi)} \alpha_{\widehat{\mathcal{D}}} A_{\widehat{\mathcal{D}}}} < \frac{\alpha_{\widehat{\mathcal{D}}_b} A_{\widehat{\mathcal{D}}_b}}{\alpha_{\widehat{\mathcal{D}}_a} A_{\widehat{\mathcal{D}}_a} + \alpha_{\widehat{\mathcal{D}}_b} A_{\widehat{\mathcal{D}}_b}},$$

311 where  $A_{\widehat{\mathcal{D}}} > 0$  denotes the volume (area) of the patch of elements in  $\widehat{\mathcal{D}}$  containing  $\xi$ .

312 Clearly,  $\delta_{\widehat{\mathcal{D}}}^\dagger(\xi) \leq 1$ . Therefore,  $\alpha_{\widehat{\mathcal{D}}_a} (\delta_{\widehat{\mathcal{D}}_b}^\dagger(\xi))^2 \leq \alpha_{\widehat{\mathcal{D}}_a}$ . Now we need to prove that

$$313 \quad (9) \quad \alpha_{\widehat{\mathcal{D}}_a} \left( \delta_{\widehat{\mathcal{D}}_b}^\dagger(\xi) \right)^2 \leq C_{\delta^\dagger} \alpha_{\widehat{\mathcal{D}}_b}.$$

314 Using (8), it is sufficient to show

$$315 \quad (10) \quad \alpha_{\widehat{\mathcal{D}}_a} \alpha_{\widehat{\mathcal{D}}_b} A_{\widehat{\mathcal{D}}_b}^2 \leq C_{\delta^\dagger} (\alpha_{\widehat{\mathcal{D}}_a} A_{\widehat{\mathcal{D}}_a} + \alpha_{\widehat{\mathcal{D}}_b} A_{\widehat{\mathcal{D}}_b})^2.$$

316 Since the mesh  $\mathcal{T}$  is quasi-uniform, elements sharing at least a point have roughly the  
 317 same volume (area). Consequently,  $A_{\widehat{\mathcal{D}}_b} \lesssim (N_{\max} - 1) A_{\widehat{\mathcal{D}}_a}$  (the worst case scenario is  
 318 when  $\widehat{\mathcal{D}}_b$  has  $N_{\max} - 1$  elements and  $\widehat{\mathcal{D}}_a$  has 1 element). Using this, we have

$$319 \quad \alpha_{\widehat{\mathcal{D}}_a} \alpha_{\widehat{\mathcal{D}}_b} A_{\widehat{\mathcal{D}}_b}^2 \lesssim (N_{\max} - 1) \alpha_{\widehat{\mathcal{D}}_a} \alpha_{\widehat{\mathcal{D}}_b} A_{\widehat{\mathcal{D}}_a} A_{\widehat{\mathcal{D}}_b} \leq \frac{N_{\max} - 1}{4} (\alpha_{\widehat{\mathcal{D}}_a} A_{\widehat{\mathcal{D}}_a} + \alpha_{\widehat{\mathcal{D}}_b} A_{\widehat{\mathcal{D}}_b})^2.$$

320 This implies (10) and we finish the proof.  $\square$

321 The definition of the set of coarse objects of  $\widehat{\mathcal{B}}$  requires further elaboration. The  
 322 set of objects  $\Lambda(\Theta_{\text{pb}})$  obtained by applying the classification in subsection 2.3 for the  
 323 PB subdomain partition  $\Theta_{\text{pb}}$  provides a classification of  $\Gamma(\Theta_{\text{pb}}) \supset \Gamma(\Theta)$ . We have the  
 324 following relation between the PB objects  $\Lambda_{\text{pb}}(\Theta)$  and the (standard) objects of the  
 325 PB partition  $\Lambda(\Theta_{\text{pb}})$ .

326 LEMMA 10. All the objects in  $\Lambda_{\text{pb}}(\Theta)$  are also in  $\Lambda(\Theta_{\text{pb}})$ , i.e.,  $\Lambda_{\text{pb}}(\Theta) \subset \Lambda(\Theta_{\text{pb}})$ .

327 *Proof.* Let us consider an object  $\lambda_{\text{pb}} \in \Lambda_{\text{pb}}(\Theta)$ . In both object partitions  $\Lambda_{\text{pb}}(\Theta)$   
 328 and  $\Lambda(\Theta_{\text{pb}})$ , we are using the same criteria, i.e.,  $\text{neigh}_{\Theta_{\text{pb}}}(\cdot)$ , to classify points. The  
 329 difference is that  $\Lambda_{\text{pb}}(\Theta)$  is the result of a classification of points in  $\Gamma(\Theta)$  whereas  
 330  $\Lambda(\Theta_{\text{pb}})$  is obtained from a classification of points in  $\Gamma(\Theta_{\text{pb}})$ . Since  $\Gamma(\Theta) \subset \Gamma(\Theta_{\text{pb}})$ ,  
 331 all points in  $\lambda_{\text{pb}}$  belong to the same object  $\lambda' \in \Lambda(\Theta_{\text{pb}})$ . Since  $\lambda_{\text{pb}}$  is on the in-  
 332 terface  $\Gamma(\Theta)$ , there exist at least two subdomains  $\widehat{\mathcal{D}}, \widehat{\mathcal{D}}' \in \text{neigh}_{\Theta_{\text{pb}}}(\lambda_{\text{pb}})$  such that  
 333  $\omega(\widehat{\mathcal{D}}) \neq \omega(\widehat{\mathcal{D}}')$ . Let us assume there is a point  $\xi \in \lambda'$  such that  $\xi \notin \lambda_{\text{pb}}$ . Then,  
 334  $\xi \in \Gamma(\Theta_{\text{pb}}) \setminus \Gamma(\Theta)$ , i.e., it only belongs to one subdomain in  $\Theta$ . As a result,  $\omega(\widehat{\mathcal{D}})$  is  
 335 the same for all  $\widehat{\mathcal{D}} \in \text{neigh}_{\Theta_{\text{pb}}}(\xi)$ . Thus, we have a contradiction, since  $\text{neigh}_{\Theta_{\text{pb}}}(\xi)$   
 336 cannot be the same as  $\text{neigh}_{\Theta_{\text{pb}}}(\lambda_{\text{pb}})$ .  $\square$

337 With the theoretical support from Lemma 10, we can define the set of coarse ob-  
 338 jects  $\widehat{\Lambda}_O$  of  $\widehat{\mathcal{B}}$  as a classification of  $\Gamma(\Theta_{\text{pb}})$  as follows. On  $\Gamma(\Theta)$ , we consider the  
 339 same set of objects  $\Lambda_O$  used in the PB-BDDC preconditioner, i.e.,  $\Lambda_C$ , or  $\Lambda_C \cup$   
 340  $\Lambda_E$ , or  $\Lambda_{\text{pb}}(\Theta)$ . For the rest of the interface  $\Gamma(\Theta_{\text{pb}}) \setminus \Gamma(\Theta)$ , we enforce *full conti-*  
 341 *nuity* among PB subdomains. It can be understood as treating all FE nodes on  
 342  $\Gamma(\Theta_{\text{pb}}) \setminus \Gamma(\Theta)$  as corners. Denote this set of objects by  $\widehat{\Lambda}^*$ , we have  $\widehat{\Lambda}_O = \Lambda_O \cup \widehat{\Lambda}^*$ .  
 343 Figure 3 illustrates the partitions and coarse objects of  $\mathcal{B}$  and  $\widehat{\mathcal{B}}$  when  $\Lambda_O = \Lambda_C \cup \Lambda_E$ .  
 344

345 *Remark 11.* By construction, the BDDC space  $\widetilde{\mathbb{V}}^{\text{pb}}$  of the auxiliary BDDC pre-  
 346 conditioner  $\widehat{\mathcal{B}}$  is identical to the BDDC space  $\widetilde{\mathbb{V}}$ , defined in (4), of the PB-BDDC  
 347 preconditioner.

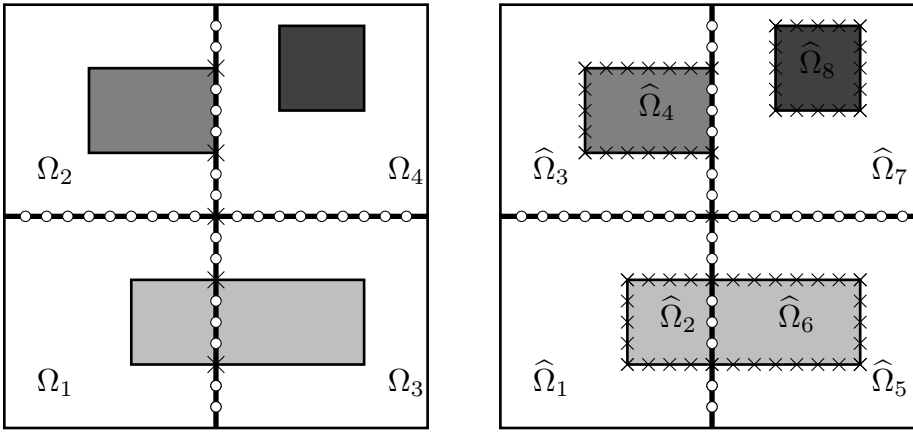


FIG. 3. Partitions and coarse objects of the PB-BDDC preconditioner  $\mathcal{B}$  (left) and the auxiliary BDDC preconditioner  $\widehat{\mathcal{B}}$  (right) when  $\Lambda_O = \Lambda_C \cup \Lambda_E$ : corner objects are labeled with crosses while nodes of other objects are labeled with circles.

348 LEMMA 12. The condition number  $\kappa(\mathcal{B}\mathcal{A})$  of the PB-BDDC preconditioned oper-  
 349 ator is bounded by

$$350 \quad (11) \quad \kappa(\mathcal{B}\mathcal{A}) \leq \max_{v \in \widetilde{\mathbb{V}}^{\text{pb}}} \frac{\langle \mathcal{A}^{\Theta_{\text{pb}}} \widehat{Q}v, \widehat{Q}v \rangle}{\langle \mathcal{A}^{\Theta_{\text{pb}}} v, v \rangle}.$$

351 *Proof.* According to [39, Theorem 15],  $\kappa(\mathcal{B}\mathcal{A})$  is bounded by

$$352 \quad (12) \quad \kappa(\mathcal{B}\mathcal{A}) \leq \max_{v \in \widetilde{\mathbb{V}}} \frac{\langle \mathcal{A}^{\Theta} Qv, Qv \rangle}{\langle \mathcal{A}^{\Theta} v, v \rangle}.$$

353 Now we only need to bound the right-hand-side in (12) by the one in (11).

On the one hand, using the fact that  $\widetilde{\mathbb{V}} = \widetilde{\mathbb{V}}^{\text{pb}}$ , we have  $\langle \mathcal{A}^{\Theta} v, v \rangle = \langle \mathcal{A}^{\Theta_{\text{pb}}} v, v \rangle$  for all  $v \in \widetilde{\mathbb{V}}$  because any  $v \in \widetilde{\mathbb{V}}$  is continuous in each subdomain of  $\Theta$ . On the other hand, let us prove that the weighting operator  $\widehat{\mathcal{W}}$  defined by (5) for  $\Theta_{\text{pb}}$  restricted to  $\mathbb{V}$  is identical to the weighting operator  $\mathcal{W}$  defined by (5) for  $\Theta$ . Let us consider a subdomain  $\mathcal{D} \in \Theta$  and its PB partition  $\Theta_{\text{pb}}(\mathcal{D})$ . We have

$$\delta_{\mathcal{D}}^{\dagger}(\xi) = \sum_{\widehat{\mathcal{D}} \in \Theta_{\text{pb}}(\mathcal{D}), \widehat{\mathcal{D}} \ni \xi} \delta_{\widehat{\mathcal{D}}}^{\dagger}(\xi),$$

354 by the definition in (5). For an arbitrary function  $v \in \mathbb{V} \subset \mathbb{V}^{\text{pb}}$ , we find that

$$\begin{aligned}
355 \quad \mathcal{W}v(\xi) &= \sum_{\mathcal{D} \in \text{neigh}_{\Theta}(\xi)} \delta_{\mathcal{D}}^{\dagger}(\xi) v_{\mathcal{D}}(\xi) = \sum_{\mathcal{D} \in \text{neigh}_{\Theta}(\xi)} \sum_{\hat{\mathcal{D}} \in \Theta_{\text{pb}}, \hat{\mathcal{D}} \ni \xi} \delta_{\hat{\mathcal{D}}}^{\dagger}(\xi) v_{\mathcal{D}}(\xi) \\
356 \quad &= \sum_{\hat{\mathcal{D}} \in \text{neigh}_{\Theta_{\text{pb}}}(\xi)} \delta_{\hat{\mathcal{D}}}^{\dagger}(\xi) v_{\hat{\mathcal{D}}}(\xi) = \widehat{\mathcal{W}}v(\xi). \\
357
\end{aligned}$$

358 Therefore,  $\widehat{\mathcal{Q}}v$  and  $\mathcal{Q}v$  are identical on  $\Gamma(\Theta)$  and  $\widehat{\mathcal{Q}}v$  is continuous across  $\Gamma(\Theta_{\text{pb}})$ . In  
359 addition,  $\mathcal{Q}v$  is discrete  $\alpha$ -harmonic in each  $\mathcal{D} \in \Theta$  and have minimal energy norm  
360 w.r.t  $\mathcal{A}^{\Theta}$ . As a consequence,

$$\begin{aligned}
361 \quad \langle \mathcal{A}^{\Theta} \mathcal{Q}v, \mathcal{Q}v \rangle &= \sum_{\mathcal{D} \in \Theta} \langle \mathcal{A}_{\mathcal{D}}^{\Theta} \mathcal{Q}v, \mathcal{Q}v \rangle \\
362 \quad &\leq \sum_{\mathcal{D} \in \Theta} \langle \mathcal{A}_{\mathcal{D}}^{\Theta} \widehat{\mathcal{Q}}v, \widehat{\mathcal{Q}}v \rangle = \sum_{\hat{\mathcal{D}} \in \Theta_{\text{pb}}} \langle \mathcal{A}_{\hat{\mathcal{D}}}^{\Theta_{\text{pb}}} \widehat{\mathcal{Q}}v, \widehat{\mathcal{Q}}v \rangle = \langle \mathcal{A}^{\Theta_{\text{pb}}} \widehat{\mathcal{Q}}v, \widehat{\mathcal{Q}}v \rangle. \\
363
\end{aligned}$$

364 This finishes the proof.  $\square$

365 We could stop here and derive the estimate for  $\kappa(\mathcal{BA})$  knowing that the condition  
366 number of the auxiliary BDDC preconditioned operator  $\widehat{\mathcal{B}}\mathcal{A}$  is estimated by an upper  
367 bound of the last quantity on the right of (12). However, we will go a bit further to  
368 obtain a stronger result.

369 LEMMA 13. Assume that  $\Lambda_O$  is such that Assumption 7 holds. Then we have the  
370 following inequality:

$$371 \quad (13) \quad \max_{v \in \widetilde{\mathbb{V}}^{\text{pb}}} \frac{\langle \mathcal{A}^{\Theta_{\text{pb}}} \widehat{\mathcal{Q}}v, \widehat{\mathcal{Q}}v \rangle}{\langle \mathcal{A}^{\Theta_{\text{pb}}} v, v \rangle} \leq C \max\{1, \text{TOL}\} \max_{\mathcal{D} \in \Theta_{\text{pb}}} \left( 1 + \log \left( \frac{H(\mathcal{D})}{h(\mathcal{D})} \right) \right)^2,$$

372 where the constant  $C$  is independent of the number of subdomains,  $H(\hat{\mathcal{D}})$ ,  $h(\hat{\mathcal{D}})$  and  
373 the physical coefficient  $\alpha$ .

374 *Proof.* By triangle inequality, we have

$$375 \quad (14) \quad \max_{v \in \widetilde{\mathbb{V}}^{\text{pb}}} \frac{\langle \mathcal{A}^{\Theta_{\text{pb}}} \widehat{\mathcal{Q}}v, \widehat{\mathcal{Q}}v \rangle}{\langle \mathcal{A}^{\Theta_{\text{pb}}} v, v \rangle} \leq 1 + \max_{v \in \widetilde{\mathbb{V}}^{\text{pb}}} \frac{\langle \mathcal{A}^{\Theta_{\text{pb}}} (\widehat{\mathcal{Q}}v - v), (\widehat{\mathcal{Q}}v - v) \rangle}{\langle \mathcal{A}^{\Theta_{\text{pb}}} v, v \rangle}.$$

376 Let  $w = \widehat{\mathcal{Q}}v - v$ . Given a FE function  $u \in \mathbb{V}_{\hat{\mathcal{D}}}$ , we denote by  $\theta_{\lambda}^{\hat{\mathcal{D}}}(u) \in \mathbb{V}_{\hat{\mathcal{D}}}$  the FE  
377 function that is discrete  $\alpha$ -harmonic in  $\hat{\mathcal{D}}$  and agrees with  $u$  at the FE nodes in the  
378 object  $\lambda$  and vanishes at all the other nodes on  $\partial\hat{\mathcal{D}}$ . Since  $\Lambda(\Theta_{\text{pb}})$  is a partition of  
379  $\Gamma(\Theta_{\text{pb}})$ , we can split  $w$  into object and subdomain contributions as follows:

$$380 \quad (15) \quad w = \sum_{\lambda \in \Lambda(\Theta_{\text{pb}})} \sum_{\hat{\mathcal{D}} \in \text{neigh}_{\Theta_{\text{pb}}}(\lambda)} \theta_{\lambda}^{\hat{\mathcal{D}}}(w).$$

381 By the construction of the set of object  $\widehat{\Lambda}_O = \Lambda_O \cup \widehat{\Lambda}^*$  and the definition of  $\widetilde{\mathbb{V}}^{\text{pb}}$ ,  $w$   
382 vanishes at all coarse objects in  $\widehat{\Lambda}^*$ , i.e, at all FE nodes in  $\Gamma(\Theta_{\text{pb}}) \setminus \Gamma(\Theta)$ . Consequently,  
383 (15) can be simplified as follows:

$$384 \quad (16) \quad w = \sum_{\lambda \in \Lambda_{\text{pb}}(\Theta)} \sum_{\hat{\mathcal{D}} \in \Theta_{\text{pb}}^{\theta}} \theta_{\lambda}^{\hat{\mathcal{D}}}(w).$$

385 When  $\Lambda_O$  satisfies [Assumption 7](#), the set of objects in  $\widehat{\Lambda}_O$  also fulfils [[50](#), Assump-  
386 tion 6.27]. Consequently, using [Lemma 9](#), we can perform an analysis similar to that  
387 in the proof [[50](#), Lemma 6.36] (see also [[31](#), Lemma 10]) to obtain

$$388 \quad \langle \mathcal{A}_{\hat{\mathcal{D}}}^{\Theta_{\text{pb}}} \theta_{\lambda}^{\hat{\mathcal{D}}}(w), \theta_{\lambda}^{\hat{\mathcal{D}}}(w) \rangle$$

$$389 \quad \leq C \max\{1, \text{TOL}\} \left( 1 + \log \left( \frac{H(\hat{\mathcal{D}})}{h(\hat{\mathcal{D}})} \right) \right)^2 \sum_{\hat{\mathcal{D}} \in \text{neigh}_{\Theta_{\text{pb}}}(\lambda)} \langle \mathcal{A}_{\hat{\mathcal{D}}}^{\Theta_{\text{pb}}} v, v \rangle$$
390

391 for any  $\hat{\mathcal{D}} \in \Theta_{\text{pb}}^{\partial}$  and  $\lambda \in \Lambda(\Theta_{\text{pb}})$ . Here the constant  $C$  is proportional to  $C_{\delta\uparrow}$  in  
392 [Lemma 9](#), but is otherwise independent of  $H(\hat{\mathcal{D}})$ ,  $h(\hat{\mathcal{D}})$  and the physical coefficient  $\alpha$ .

393 Adding up the estimate for all subdomain  $\hat{\mathcal{D}} \in \Theta_{\text{pb}}$ , we find that

$$394 \quad (17) \quad \langle \mathcal{A}^{\Theta_{\text{pb}}} w, w \rangle \leq C \max\{1, \text{TOL}\} \max_{\hat{\mathcal{D}} \in \Theta_{\text{pb}}^{\partial}} \left( 1 + \log \left( \frac{H(\hat{\mathcal{D}})}{h(\hat{\mathcal{D}})} \right) \right)^2 \langle \mathcal{A}^{\Theta_{\text{pb}}} v, v \rangle.$$

395 This finishes the proof.  $\square$

396 Combining results in [Lemma 12](#) and [Lemma 13](#), we have the final bound for  
397 the PB-BDDC preconditioner, which is both weakly scalable and independent of the  
398 coefficient  $\alpha$ .

399 **THEOREM 14.** *The condition number of the PB-BDDC preconditioned operator*  
400  *$\kappa(\mathcal{BA})$  is bounded by*

$$401 \quad \kappa(\mathcal{BA}) \leq C \max\{1, \text{TOL}\} \max_{\hat{\mathcal{D}} \in \Theta_{\text{pb}}^{\partial}} \left( 1 + \log \left( \frac{H(\hat{\mathcal{D}})}{h(\hat{\mathcal{D}})} \right) \right)^2,$$

402 where the constant  $C$  is independent of the number of subdomains,  $H(\hat{\mathcal{D}})$ ,  $h(\hat{\mathcal{D}})$  and  
403 the physical coefficient  $\alpha$ .

404 *Remark 15.* As seen in the [Lemma 13](#) and [Theorem 14](#), the condition number  
405 associated with the PB-BDDC method depends only on the characteristic size and  
406 mesh size of PB subdomains touching the original interface  $\Gamma(\Theta)$ . Further, the con-  
407 vergence of the PB-BDDC is independent of variations of the coefficient. The main  
408 target of this work is achieved.

409 **3.5. Relaxed physics-based BDDC.** The definition of the coarse objects for  
410 the PB-BDDC preconditioner, based on the requirement that the coefficient has to  
411 be constant in each PB subdomain, can result in a large coarse space. That is the  
412 case for heterogeneous problems where the physical coefficient varies across a wide  
413 spectrum of values in a small spatial scale.

414 In order to deal with a more general class of problems, we propose the relaxed PB-  
415 BDDC preconditioner (rPB-BDDC) where we only require that the maximal contrast  
416 in each PB subdomain is less than some predefined tolerance  $r$ . We consider a relaxed  
417 PB partition  $\Theta^{\text{pb}}$  such that

$$418 \quad (18) \quad \max_{\tau, \tau' \subset \hat{\mathcal{D}}} \frac{\alpha_{\tau}}{\alpha_{\tau'}} \leq r, \quad \text{for any } \hat{\mathcal{D}} \in \Theta^{\text{pb}}.$$

419 Here the threshold  $r$  is equal or greater than 1. This way, we can control the size of  
420 the coarse problem and the condition number bounds with the choice of  $r$ .

421 As the coefficient is no longer constant in each PB subdomain, we need to use  
 422 a weighted-constraint in the definition of coarse DOFs. More specifically, instead of  
 423 using (3), we use

$$424 \quad (19) \quad c_\lambda^{\mathcal{D}}(u) \doteq \frac{\int_\lambda \bar{\alpha} u ds}{\int_\lambda \bar{\alpha} 1 ds}, \quad \text{where } \bar{\alpha}(\xi) \doteq \max_{\tau \in \mathcal{T}, \tau \ni \xi} \alpha_\tau.$$

425

426 *Remark 16.* The larger  $r$  becomes the smaller the size of the coarse problem of the  
 427 rPB-BDDC preconditioner is and the larger its condition number grows to. When  
 428  $r = 1$  the rPB-BDDC preconditioner becomes the PB-BDDC preconditioner. By  
 429 tuning the threshold  $r$ , one can obtain a right balance between the time spent on  
 430 setting up the preconditioner (especially in forming the coarse space) and the time  
 431 spent on applying the preconditioner in a Krylov solver. The optimal threshold is of  
 432 course problem dependent. However, finding a good threshold is not tricky. This is  
 433 illustrated in section 4.

434 *Remark 17.* The rPB-BDDC preconditioner makes use of a threshold. This is sim-  
 435 ilar to the adaptive coarse space approach where only eigenfunctions associated with  
 436 eigenvalues below a predefined threshold are included in the coarse space. However,  
 437 the rPB-BDDC preconditioner does not involve any eigenvalue or auxiliary problems  
 438 and is far simpler and cheaper.

439 **4. Numerical experiments.** In this section, we test the robustness and effi-  
 440 ciency of the PB-BDDC and rPB-BDDC preconditioners for the system matrix asso-  
 441 ciated with (2) for different types of variation in the coefficient  $\alpha$ , which are similar  
 442 but generally harder than the ones in [42, 28, 36].

443 Due to the difficulty of heterogeneous problems, in PB-BDDC and rPB-BDDC  
 444 methods, we tend to use a large number of objects. Many of them are not corners. In  
 445 all tested cases, these objects are enough to make the local Neumann problems and  
 446 global coarse problem well-posed and we can optionally drop corner objects. No corner  
 447 detection mechanism (see, e.g, [46]) has been needed in any tested case. Alternatively,  
 448 one might want to consider the perturbed formulation introduced in [7, 8]. However,  
 449 this approach has not been extended to heterogeneous problems yet.

450 In all of the experiments, we consider the physical domain  $\Omega = (0, 1)^2$ . Unless  
 451 stated otherwise, we use the uniform triangular meshes of size  $h = 1/72$  and the  
 452 regular  $3 \times 3$  subdomain partition. In all cases, we report the dimension of the  
 453 coarse space, denoted by  $\dim$ , and the number of iterations required for the conjugate  
 454 gradient method to reduce the residual norm by a factor of  $10^6$ . We also provide the  
 455 condition number  $\kappa$  in most examples.

456 **4.1. Two channels.** In this test case, we consider two channels of high  $\alpha$  cutting  
 457 through vertical subdomain edges (see Figure 4). The coefficient in the channels  $\alpha_{\max}$   
 458 takes the values  $\{10^2, 10^4, 10^6, 10^8\}$ , while the coefficient in the rest of the domain is  
 459 equal to 1.

460 From Table 1, we can see that the condition number and the number of iter-  
 461 ations for the standard BDDC preconditioner (BDDC(ce)) definitely increase with  
 462  $\alpha_{\max}$ , whereas they remain practically constant for both variants of the PB-BDDC  
 463 preconditioners (PB-BDDC(ce) and PB-BDDC(e)). In other words, the convergence  
 464 of the PB-BDDC method is independent of the contrast and the PB-BDDC method is  
 465 perfectly robust for this test case. Figure 4 shows the coarse objects of PB-BDDC(ce)  
 466 on the interface of the partition.

TABLE 1  
Comparison of the iteration count and condition number in the two channels test case.

dim $\rightarrow$	BDDC(ce)		PB-BDDC(ce)		PB-BDDC(e)	
	16		64		36	
$\alpha_{\max}$	# it.	$\kappa$	# it.	$\kappa$	# it.	$\kappa$
$10^2$	21	2.12e3	10	5.47e0	13	1.20e1
$10^4$	28	2.87e5	10	5.31e0	14	1.21e1
$10^6$	44	2.89e7	10	5.31e0	15	1.21e1
$10^8$	64	3.88e9	10	5.31e0	15	1.21e1

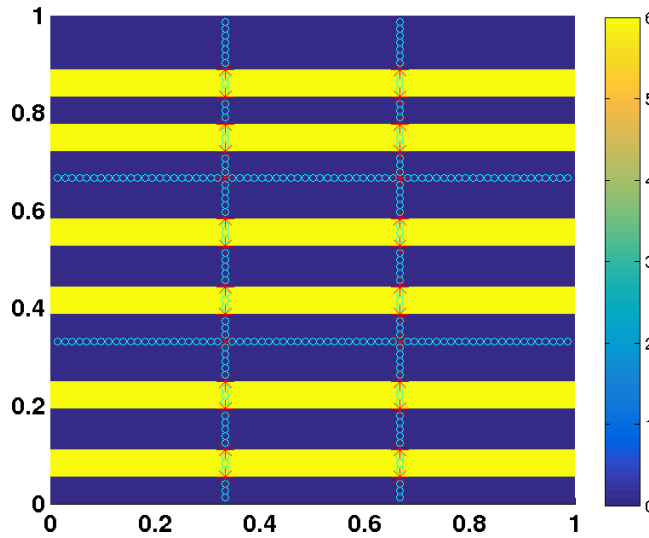


FIG. 4. Distribution of the coefficient in the two-channels test case when  $\alpha_{\max} = 10^6$ . The coarse objects of PB-BDDC(ce) are shown on the interface with corners labeled by stars and DOFs in edges labeled by circles.

467 **4.2. Channels and inclusions.** In this test case, we consider both channels  
468 and inclusions of high coefficient. First, the three channels include all the elements  
469 whose centroids are less than  $2 \cdot 10^{-2}$  from one of the following three lines:

$$\begin{aligned}
470 \quad & L1 : x_1 - x_2 - 0.2 = 0, \\
471 \quad & L2 : x_1 + x_2 - 0.7 = 0, \\
472 \quad & L3 : x_1 - 0.7x_2 - 0.7 = 0.
\end{aligned}$$

474 The coefficient  $\alpha_{\max}$  in these channels takes the values  $\{10^2, 10^4, 10^6, 10^8\}$ . Secondly,  
475 the inclusions are defined as the regions of elements whose all vertices  $x$  satisfy

$$476 \quad \text{mod}(\text{floor}(10x_i), 2) = 1, \text{ for } i = 1, 2.$$

477 For an element  $\tau$  that belongs to one of the inclusions and is not in the channels, its  
478 coefficient is defined as

$$479 \quad (20) \quad \alpha|_{\tau} = (\alpha_{\max}/10)^{1/5 * \text{floor}(0.5 * \text{floor}(10x_1(c_{\tau})) + 1)}, \quad \text{where } c_{\tau} \text{ is the centroid of } \tau.$$

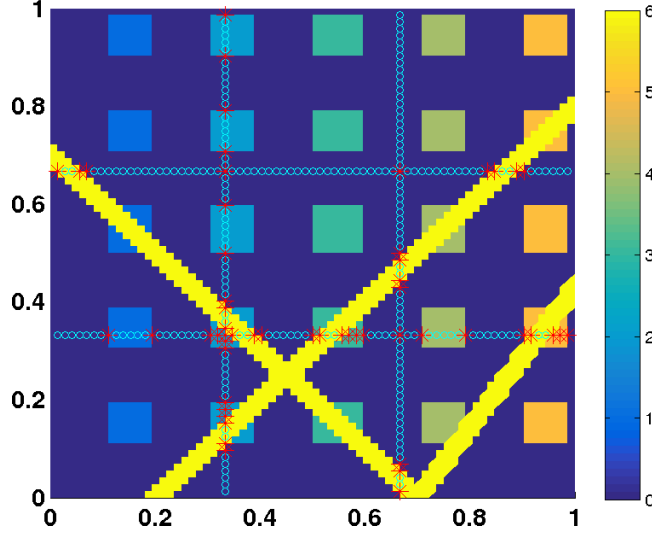


FIG. 5. Distribution of the coefficient for the channels and inclusions test case when  $\alpha_{\max} = 10^6$ . The coarse objects of PB-BDDC(ce) are shown on the interface with corners labeled by stars and DOFs in edges labeled by circles.

480 The coefficient in (20) is: a) constant in each inclusion b) increasing from left to right  
 481 c) increasing as  $\alpha_{\max}$  increases and d) always belongs to  $(1, \alpha_{\max})$ . For the rest of the  
 482 domain, we set  $\alpha = 1$ . The maximal contrast ratio in this experiment is  $10^8$ .

483 We can see from Table 2 that as  $\alpha_{\max}$  becomes larger the condition number and  
 484 the number of iterations associated with the standard BDDC(ce) method increases  
 485 significantly. In contrast, both variant of the PB-BDDC methods, PB-BDDC(ce) and  
 486 PB-BDDC(e), are perfectly robust with respect to the changes of the coefficient in  
 487 the channels and in the inclusions. Especially, PB-BDDC(e) maintains its robustness  
 488 with a reasonably small coarse space.

TABLE 2

Comparison of the iteration count and condition number in the channels and inclusions test case.

dim $\rightarrow$	BDDC(ce)		PB-BDDC(ce)		PB-BDDC(e)	
	16		89		39	
$\alpha_{\max}$	# it.	$\kappa$	# it.	$\kappa$	# it.	$\kappa$
$10^2$	23	1.48e3	13	1.01e1	14	5.71e1
$10^4$	45	8.33e4	13	8.93e0	15	8.08e1
$10^6$	82	6.02e6	13	8.79e0	15	8.15e1
$10^8$	97	5.30e8	13	8.76e0	15	8.15e1

489 **4.3. Complex channels.** In this test case, we demonstrate the importance of  
 490 having acceptable paths. We consider a distribution with multiple channels of high  
 491 coefficient  $\alpha_{\max}$  taking values in  $\{10^2, 10^4, 10^6, 10^8\}$  (see Figure 6 for the case when  
 492  $\alpha_{\max} = 10^6$ ).

493 From Table 3, we can see that PB-BDDC(ce) is perfectly robust. On the other  
 494 hand, the condition number and number of iterations of the PB-BDDC(e) precon-

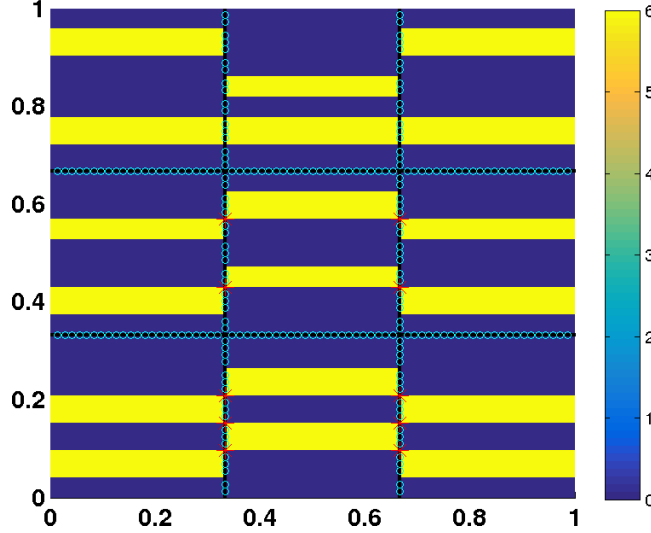


FIG. 6. Distribution of the coefficient in the complex channels test case. The coarse objects of PB-BDDC([c]e) are shown on the interface with corners labeled by stars and DOFs in edges labeled by circles. Only few corners are required to guarantee perfect robustness (to have acceptable paths).

495 conditioner increase significantly as  $\alpha_{\max}$  increases. The reason is that there are some  
 496 pairs of channels share a corner but not an edge. In PB-BDDC(e), none of these  
 497 corners are selected as a coarse objects. Consequently, there is no acceptable path  
 498 with TOL independent of the contrast between the associated paired of channels (PB  
 499 subdomains) and Assumption 7 does not hold. By including a small number of these  
 500 critical corners (represented by stars in Figure 6) in order to satisfy Assumption 7, the  
 501 resulting preconditioner, labeled PB-BDDC([c]e), is perfectly robust w.r.t changes in  
 502 the contrast of the coefficient (see Table 3).

TABLE 3  
 Comparison of the iteration count and condition number in the complex channels test case.

dim	BDDC(ce)	PB-BDDC(ce)	PB-BDDC(e)	PB-BDDC([c]e)
$\alpha_{\max}$	# it. ( $\kappa$ )			
$10^2$	22 (2.99e3)	12 (6.09e0)	19 (1.25e3)	13 (1.21e1)
$10^4$	43 (3.82e5)	12 (5.94e0)	34 (1.62e5)	13 (1.27e1)
$10^6$	70 (3.83e7)	12 (5.94e0)	51 (1.63e7)	13 (1.27e1)
$10^8$	95 (6.45e9)	12 (5.94e0)	99 (1.63e9)	13 (1.27e1)

503 **4.4. Sinusoidal variation.** In this experiment, we consider a coefficient that  
 504 varies like a sinusoid. We use a finer uniform triangular mesh of size  $h = 1/144$ . For  
 505 an element  $\tau \in \mathcal{T}$ , the coefficient  $\alpha_\tau$  is defined by

$$506 \quad \log_{10}(\alpha_\tau) = \kappa \sin(w\pi(x_1(c_\tau) + x_2(c_\tau))) + \alpha_{\text{shift}},$$

507 where  $\kappa = 3$ ,  $w = 14$ , and  $c_\tau$  is the the centroid of  $\tau$ . We note that when  $\kappa$  and/or  
 508  $w$  become larger the problem is more difficult. The distribution when  $\alpha_{\text{shift}} = 0$  is

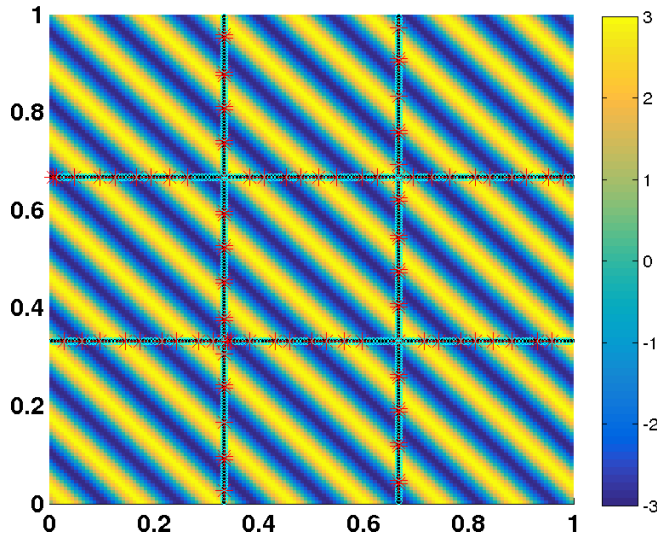


FIG. 7. Distribution of the coefficient mimicking sin function. The coarse objects of rPB-BDDC(ce) with  $r = 10^3$  are shown on the interface with corners labeled by stars and DOFs in edges labeled by circles.

509 shown in Figure 7. It is as if there are many channels going through subdomain edges  
 510 at the same time.

511 In this test case, the coefficient varies very rapidly. We test the standard BDDC  
 512 method and the rPB-BDDC method introduced in subsection 3.5, by allowing the  
 513 upper bound  $r$  for the maximal contrast in each PB subdomain to vary among  
 514  $\{10^1, 10^2, 10^3\}$ . Only iteration counts are reported as the condition number estimation  
 515 becomes too expensive for the mesh being used.

516 This is a difficult problem and the standard BDDC(ce) method requires almost  
 517 a hundred iterations to converge (see Table 4). The relaxed physics-based methods,  
 518 rPB-BDDC(ce) and rPB-BDDC(e), are able to significantly reduce the number of  
 519 iterations. That comes with the cost of solving larger coarse problems. However, by  
 520 using a suitable threshold  $r$ , we can obtain a decent preconditioner, e.g. rPB-BDDC(e)  
 521 with  $r = 10^3$ , which requires only 11 iterations using a reasonably small coarse space  
 522 of size 64. In addition, the rPB-BDDC method is also perfectly robust with shifting  
 523 in the value of the coefficient. The iteration count does not change when  $\alpha_{\text{shift}}$  takes  
 524 values in  $\{0, 6\}$ .

TABLE 4  
 Comparison of the iteration count in the continuous sin test case.

		BDDC(ce)	rPB-BDDC(ce)			rPB-BDDC(e)		
$r$			10	$10^2$	$10^3$	10	$10^2$	$10^3$
	dim	16	474	292	188	212	116	64
$\alpha_{\text{shift}} = 0$	# it.	92	7	10	11	10	12	11
$\alpha_{\text{shift}} = 6$	# it.	99	7	10	11	10	12	11

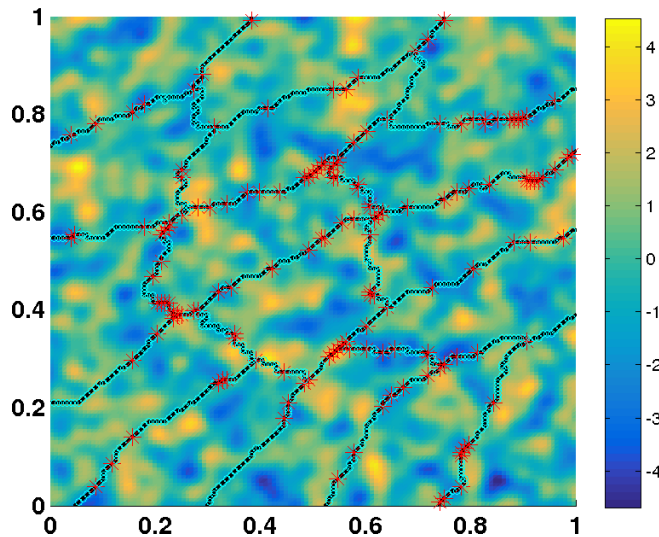


FIG. 8. *Distribution of the coefficient in the log-normal test case. The coarse objects of rPB-BDDC(ce) with  $r = 10^2$  are shown on the interface with corners labeled by stars and DOFs in edges labeled by circles.*

525 **4.5. Log-Normal.** In this test case, we test the performance of the rPB-BDDC  
 526 method for a log-normal distribution of the coefficient. This type of distribution is  
 527 particularly important for geoscience and petroleum engineering applications. We  
 528 consider  $\alpha_{\text{cont}}(x, w) = 10^{Z(x, w)}$ , where  $Z(x, w)$  is a Gaussian random field with zero  
 529 mean and Gaussian covariance

$$530 \quad C(x, y) = \sigma^2 \exp\left(-\frac{\|x - y\|^2}{\ell^2}\right), \quad \text{with } \sigma = 1.5, \ell^2 = 1e-3.$$

531 For this experiment, a uniform triangular mesh of size  $h = 1/128$  is utilized. Using the  
 532 spectral decomposition method described in [37], we are able to obtain a realization  
 533 of  $\alpha_{\text{cont}}(x, w)$  at mesh vertices. The piecewise coefficient  $\alpha_\tau$  on an element  $\tau$  is then  
 534 defined as the average of  $\alpha_{\text{cont}}(x, w)$  at the three vertices. The distribution of  $\alpha$  with  
 535 a partition obtained from METIS [26] is shown in Figure 8. The contrast ratio in this  
 536 test case is nearly  $10^{10}$ . The coarse objects of rPB-BDDC(ce) when  $r = 10^2$  are also  
 537 illustrated.

538 In Table 5, we can see that, compared to the standard BDDC(ce) method, rPB-  
 539 BDDC(ce) and rPB-BDDC(e) preconditioners require much fewer iterations to con-  
 540 verge. They, however, have a larger coarse space. By adjusting the threshold for the  
 541 maximal contrast in each object, we can reduce the size of the coarse space while  
 542 maintaining a reasonably fast convergence. This is clearly illustrated in Table 5.

543 **5. Conclusions.** In this work, we have proposed a novel type of BDDC pre-  
 544 conditioner that are robust for heterogeneous problems with high contrast. The  
 545 underlying idea is to modify the continuity constraints enforced among subdomains  
 546 making use of the knowledge about the physical coefficients. In order to do that, we  
 547 rely on a physically motivated partition of standard coarse objects (corners, edges, and  
 548 faces) into coarse sub-objects. The motivation for that is the well-known robustness  
 549 of DD methods when there are only jumps of physical coefficients across the interface  
 550 between subdomains. All these ideas can also be used in the frame of FETI methods.

TABLE 5  
Comparison of the iteration count in the log-normal test case.

$r$	BDDC(ce)	rPB-BDDC(ce)			rPB-BDDC(e)		
		10	$10^2$	$5 \cdot 10^3$	10	$10^2$	$5 \cdot 10^3$
dim	49	488	284	239	204	127	105
# it.	77	16	25	28	25	29	33

551 In cases where the physical coefficient is constant in each coarse sub-object, we  
 552 are able to prove that the associated condition number can be bounded independent  
 553 of the number of the subdomains and the contrast of the physical coefficient. In other  
 554 words, the new preconditioner is scalable and robust for heterogeneous problems.

555 Apart from the new set of coarse objects and a new weighting operator, the (r)PB-  
 556 BDDC preconditioners are very much the same as the standard BDDC preconditioner.  
 557 As a result, the implementation of the new preconditioners involve a very simple  
 558 modification of the standard BDDC implementation. In all of our experiments, the  
 559 new preconditioners deliver fast, robust and contrast-independent convergence while  
 560 maintaining the simplicity of BDDC methods at a reasonable computational cost.  
 561 Compared to the other robust DD solvers for heterogeneous problems currently avail-  
 562 able, such as the ones in [25, 45, 25, 43, 44, 22, 23, 42, 47, 15, 49, 48, 28, 27, 29, 36, 24],  
 563 our new methods do not involve any type of eigenvalue or auxiliary problems.

564 For further work, we want to implement the new preconditioners in the extremely  
 565 scalable BDDC code in FEMPAR [3, 4, 5, 6]. The multilevel extension and the task-  
 566 overlapping implementation are particularly interesting in the (r)PB-BDDC case due  
 567 to generally larger coarse problem. With such extremely scalable implementation, we  
 568 are interested in applying our new preconditioners to realistic 3D problems, e.g., in  
 569 geoscience applications.

#### REFERENCES

- [1] A. ABDULLE, W. E. B. ENGQUIST, AND E. VANDEN-EIJNDEN, *The heterogeneous multiscale method*, Acta Numer., 21 (2012), pp. 1–87.
- [2] S. BADIA, A. F. MARTÍN, AND J. PRINCIPE, *Enhanced balancing Neumann-Neumann preconditioning in computational fluid and solid mechanics*, International Journal for Numerical Methods in Engineering, 96 (2013), pp. 203–230, <http://dx.doi.org/10.1002/nme.4541>.
- [3] S. BADIA, A. F. MARTÍN, AND J. PRINCIPE, *Implementation and scalability analysis of balancing domain decomposition methods*, Archives of Computational Methods in Engineering, 20 (2013), pp. 239–262, <http://dx.doi.org/10.1007/s11831-013-9086-4>.
- [4] S. BADIA, A. F. MARTÍN, AND J. PRINCIPE, *A highly scalable parallel implementation of balancing domain decomposition by constraints*, SIAM Journal on Scientific Computing, 36 (2014), pp. C190–C218, <http://dx.doi.org/10.1137/130931989>.
- [5] S. BADIA, A. F. MARTÍN, AND J. PRINCIPE, *On the scalability of inexact balancing domain decomposition by constraints with overlapped coarse/fine corrections*, Parallel Computing, 50 (2015), pp. 1 – 24, <http://dx.doi.org/10.1016/j.parco.2015.09.004>.
- [6] S. BADIA, A. F. MARTÍN, AND J. PRINCIPE, *Multilevel balancing domain decomposition at extreme scales*, SIAM J. Sci. Comput., 38 (2016), pp. C22–C52, <http://dx.doi.org/10.1137/15M1013511>.
- [7] S. BADIA AND H. NGUYEN, *Relaxing the roles of corners in bddc by perturbed formulation*, in Domain decomposition methods in science and engineering XXIII, Lect. Notes Comput. Sci. Eng., Springer, Heidelberg, accepted.
- [8] S. BADIA AND H. NGUYEN, *Balancing domain decomposition by perturbation*, (submitted).
- [9] S. C. BRENNER AND L. R. SCOTT, *The mathematical theory of finite element methods*, vol. 15 of Texts in Applied Mathematics, Springer, New York, third ed., 2008, <http://dx.doi.org/>

- 10.1007/978-0-387-75934-0.
- [10] S. C. BRENNER AND L.-Y. SUNG, *BDDC and FETI-DP without matrices or vectors*, Computer Methods in Applied Mechanics and Engineering, 196 (2007), pp. 1429–1435, <http://dx.doi.org/10.1016/j.cma.2006.03.012>.
  - [11] T. F. CHAN AND T. P. MATHEW, *Domain decomposition algorithms*, Acta numerica, 3 (1994), pp. 61–143.
  - [12] C. R. DOHRMANN, *A Preconditioner for Substructuring Based on Constrained Energy Minimization*, SIAM Journal on Scientific Computing, 25 (2003), pp. 246–258, <http://dx.doi.org/10.1137/S1064827502412887>.
  - [13] C. R. DOHRMANN, *An approximate BDDC preconditioner*, Numerical Linear Algebra with Applications, 14 (2007), pp. 149–168, <http://dx.doi.org/10.1002/nla.514>.
  - [14] C. R. DOHRMANN AND O. B. WIDLUND, *A BDDC algorithm with deluxe scaling for three-dimensional  $H(\text{curl})$  problems*, Communications on Pure and Applied Mathematics, 69 (2016), pp. 745–770, <http://dx.doi.org/10.1002/cpa.21574>.
  - [15] V. DOLEAN, F. NATAF, R. SCHEICHL, AND N. SPILLANE, *Analysis of a two-level Schwarz method with coarse spaces based on local Dirichlet-to-Neumann maps*, Comput. Methods Appl. Math., 12 (2012), pp. 391–414, <http://dx.doi.org/10.2478/cmam-2012-0027>.
  - [16] M. DRYJA, J. GALVIS, AND M. SARKIS, *BDDC methods for discontinuous Galerkin discretization of elliptic problems*, J. Complexity, 23 (2007), pp. 715–739, <http://dx.doi.org/10.1016/j.jco.2007.02.003>.
  - [17] M. DRYJA, M. V. SARKIS, AND O. B. WIDLUND, *Multilevel Schwarz methods for elliptic problems with discontinuous coefficients in three dimensions*, Numer. Math., 72 (1996), pp. 313–348, <http://dx.doi.org/10.1007/s002110050172>.
  - [18] M. DRYJA, B. F. SMITH, AND O. B. WIDLUND, *Schwarz analysis of iterative substructuring algorithms for elliptic problems in three dimensions*, SIAM J. Numer. Anal., 31 (1994), pp. 1662–1694, <http://dx.doi.org/10.1137/0731086>.
  - [19] W. E, B. ENGQUIST, X. LI, W. REN, AND E. VANDEN-ELJNDEN, *Heterogeneous multiscale methods: a review*, Commun. Comput. Phys., 2 (2007), pp. 367–450.
  - [20] C. FARHAT, M. LESOINNE, P. LE TALLEC, K. PIERSON, AND D. RIXEN, *FETI-DP: a dual-primal unified FETI method-part I: A faster alternative to the two-level FETI method*, International Journal for Numerical Methods in Engineering, 50 (2001), pp. 1523–1544, <http://dx.doi.org/10.1002/nme.76>.
  - [21] C. FARHAT, M. LESOINNE, AND K. PIERSON, *A scalable dual-primal domain decomposition method*, Numerical Linear Algebra with Applications, 7 (2000), pp. 687–714, [http://dx.doi.org/10.1002/1099-1506\(200010/12\)7:7/8<687::AID-NLA219>3.0.CO;2-S](http://dx.doi.org/10.1002/1099-1506(200010/12)7:7/8<687::AID-NLA219>3.0.CO;2-S).
  - [22] J. GALVIS AND Y. EFENDIEV, *Domain decomposition preconditioners for multiscale flows in high-contrast media*, Multiscale Model. Simul., 8 (2010), pp. 1461–1483, <http://dx.doi.org/10.1137/090751190>.
  - [23] J. GALVIS AND Y. EFENDIEV, *Domain decomposition preconditioners for multiscale flows in high contrast media: reduced dimension coarse spaces*, Multiscale Model. Simul., 8 (2010), pp. 1621–1644, <http://dx.doi.org/10.1137/100790112>.
  - [24] M. J. GANDER, A. LONELAND, AND T. RAHMAN, *Analysis of a new harmonically enriched multiscale coarse space for domain decomposition methods*, Dec. 2015, [arXiv:1512.05285 \[math.NA\]](https://arxiv.org/abs/1512.05285).
  - [25] I. G. GRAHAM, P. O. LECHNER, AND R. SCHEICHL, *Domain decomposition for multiscale PDEs*, Numer. Math., 106 (2007), pp. 589–626, <http://dx.doi.org/10.1007/s00211-007-0074-1>.
  - [26] G. KARYPIS AND V. KUMAR, *A fast and high quality multilevel scheme for partitioning irregular graphs*, SIAM J. Sci. Comput., 20 (1998), pp. 359–392 (electronic), <http://dx.doi.org/10.1137/S1064827595287997>.
  - [27] H. H. KIM AND E. T. CHUNG, *A BDDC algorithm with enriched coarse spaces for two-dimensional elliptic problems with oscillatory and high contrast coefficients*, Multiscale Model. Simul., 13 (2015), pp. 571–593, <http://dx.doi.org/10.1137/140970598>.
  - [28] A. KLAWONN, P. RADTKE, AND O. RHEINBACH, *FETI-DP methods with an adaptive coarse space*, SIAM Journal on Numerical Analysis, 53 (2015), pp. 297–320, <http://dx.doi.org/10.1137/130939675>.
  - [29] A. KLAWONN, P. RADTKE, AND O. RHEINBACH, *Adaptive coarse spaces for bddc with a transformation of basis*, in Domain Decomposition Methods in Science and Engineering XXII, T. Dickopf, J. M. Gander, L. Halpern, R. Krause, and F. L. Pavarino, eds., Springer International Publishing, 2016, pp. 301–309, [http://dx.doi.org/10.1007/978-3-319-18827-0\\_29](http://dx.doi.org/10.1007/978-3-319-18827-0_29).
  - [30] A. KLAWONN AND O. B. WIDLUND, *Dual-primal FETI methods for linear elasticity*, Communications on Pure and Applied Mathematics, 59 (2006), pp. 1523–1572, <http://dx.doi.org/10.1002/cpa.20156>.

- [31] A. KLAWONN, O. B. WIDLUND, AND M. DRYJA, *Dual-primal FETI methods for three-dimensional elliptic problems with heterogeneous coefficients*, SIAM J. Numer. Anal., 40 (2002), pp. 159–179 (electronic), <http://dx.doi.org/10.1137/S0036142901388081>.
- [32] A. KLAWONN, O. B. WIDLUND, AND M. DRYJA, *Dual-primal FETI methods with face constraints*, in Recent developments in domain decomposition methods (Zürich, 2001), vol. 23 of Lect. Notes Comput. Sci. Eng., Springer, Berlin, 2002, pp. 27–40, [http://dx.doi.org/10.1007/978-3-642-56118-4\\_2](http://dx.doi.org/10.1007/978-3-642-56118-4_2).
- [33] J. H. LEE, *A balancing domain decomposition by constraints deluxe method for Reissner-Mindlin plates with Falk-Tu elements*, SIAM J. Numer. Anal., 53 (2015), pp. 63–81, <http://dx.doi.org/10.1137/130940669>.
- [34] J. LI AND O. B. WIDLUND, *FETI-DP, BDDC, and block Cholesky methods*, International Journal for Numerical Methods in Engineering, 66 (2006), pp. 250–271, <http://dx.doi.org/10.1002/nme.1553>.
- [35] J. LI AND O. B. WIDLUND, *On the use of inexact subdomain solvers for BDDC algorithms*, Computer Methods in Applied Mechanics and Engineering, 196 (2007), pp. 1415–1428, <http://dx.doi.org/10.1016/j.cma.2006.03.011>.
- [36] S. LOISEL, H. NGUYEN, AND R. SCHEICHL, *Optimized schwarz and 2-lagrange multiplier methods for multiscale elliptic pdes*, SIAM Journal on Scientific Computing, 37 (2015), pp. A2896–A2923, <http://dx.doi.org/10.1137/15M1009676>.
- [37] G. J. LORD, C. E. POWELL, AND T. SHARDLOW, *An Introduction to Computational Stochastic PDEs*, Cambridge Texts in Applied Mathematics, 2014.
- [38] J. MANDEL, *Balancing domain decomposition*, Communications in Numerical Methods in Engineering, 9 (1993), pp. 233–241, <http://dx.doi.org/10.1002/cnm.1640090307>.
- [39] J. MANDEL AND C. R. DOHRMANN, *Convergence of a balancing domain decomposition by constraints and energy minimization*, Numerical Linear Algebra with Applications, 10 (2003), pp. 639–659, <http://dx.doi.org/10.1002/nla.341>.
- [40] J. MANDEL, B. SOUSEDÍK, AND C. DOHRMANN, *Multispace and multilevel BDDC*, Computing, 83 (2008), pp. 55–85, <http://dx.doi.org/10.1007/s00607-008-0014-7>.
- [41] T. P. A. MATHEW, *Domain decomposition methods for the numerical solution of partial differential equations*, vol. 61, Springer, 2008.
- [42] F. NATAF, H. XIANG, V. DOLEAN, AND N. SPILLANE, *A coarse space construction based on local Dirichlet-to-Neumann maps*, SIAM J. Sci. Comput., 33 (2011), pp. 1623–1642, <http://dx.doi.org/10.1137/100796376>.
- [43] C. PECHSTEIN AND R. SCHEICHL, *Analysis of FETI methods for multiscale PDEs*, Numer. Math., 111 (2008), pp. 293–333, <http://dx.doi.org/10.1007/s00211-008-0186-2>.
- [44] C. PECHSTEIN AND R. SCHEICHL, *Analysis of FETI methods for multiscale PDEs. Part II: interface variation*, Numer. Math., 118 (2011), pp. 485–529, <http://dx.doi.org/10.1007/s00211-011-0359-2>.
- [45] R. SCHEICHL AND E. VAINIKKO, *Additive Schwarz with aggregation-based coarsening for elliptic problems with highly variable coefficients*, Computing, 80 (2007), pp. 319–343, <http://dx.doi.org/10.1007/s00607-007-0237-z>.
- [46] J. ŠÍSTEK, M. ČERTÍKOVÁ, P. BURDA, AND J. NOVOTNÝ, *Face-based selection of corners in 3D substructuring*, Math. Comput. Simulation, 82 (2012), pp. 1799–1811, <http://dx.doi.org/10.1016/j.matcom.2011.06.007>.
- [47] N. SPILLANE, V. DOLEAN, P. HAURET, F. NATAF, C. PECHSTEIN, AND R. SCHEICHL, *A robust two-level domain decomposition preconditioner for systems of PDEs*, C. R. Math. Acad. Sci. Paris, 349 (2011), pp. 1255–1259, <http://dx.doi.org/10.1016/j.crma.2011.10.021>.
- [48] N. SPILLANE, V. DOLEAN, P. HAURET, F. NATAF, C. PECHSTEIN, AND R. SCHEICHL, *Abstract robust coarse spaces for systems of PDEs via generalized eigenproblems in the overlaps*, Numer. Math., 126 (2014), pp. 741–770, <http://dx.doi.org/10.1007/s00211-013-0576-y>.
- [49] N. SPILLANE, V. DOLEAN, P. HAURET, F. NATAF, AND D. J. RIXEN, *Solving generalized eigenvalue problems on the interfaces to build a robust two-level FETI method*, C. R. Math. Acad. Sci. Paris, 351 (2013), pp. 197–201, <http://dx.doi.org/10.1016/j.crma.2013.03.010>.
- [50] A. TOSELLI AND O. WIDLUND, *Domain decomposition methods—algorithms and theory*, vol. 34 of Springer Series in Computational Mathematics, Springer-Verlag, Berlin, 2005.
- [51] X. TU, *Three-Level BDDC in Three Dimensions*, SIAM Journal on Scientific Computing, 29 (2007), pp. 1759–1780, <http://dx.doi.org/10.1137/050629902>.
- [52] O. B. WIDLUND AND C. R. DOHRMANN, *Domain Decomposition Methods in Science and Engineering XXII*, Springer International Publishing, Cham, 2016, ch. BDDC Deluxe Domain Decomposition, pp. 93–103, [http://dx.doi.org/10.1007/978-3-319-18827-0\\_8](http://dx.doi.org/10.1007/978-3-319-18827-0_8).
- [53] Y. ZHU, *Domain decomposition preconditioners for elliptic equations with jump coefficients*, Numer. Linear Algebra Appl., 15 (2008), pp. 271–289, <http://dx.doi.org/10.1002/nla.566>.